Robotica (2006) volume 24, pp. 273–293. © 2005 Cambridge University Press
doi:10.1017/S0263574705002110 Printed in the United Kingdom

Emergence of a dynamic pattern in wall-bouncing juggling: self-organized timing selection for rhythmic movement

Hiroaki Hirai* and Fumio Miyazaki†

(Received in Final Form: June 14, 2005, first published online 17 November 2005)

SUMMARY

This paper describes a hierarchical architecture for rhythmic movement generation, which suits a juggling-like task involving sensory-motor coordination. Our approach, which is interpreted as a "bidirectional weak coupling" to the environment, does not require a continuous monitoring of the environment, but can adapt a robot to a change in the environment, owing to the interaction between the robot and the environment at the ball contact. The proposed architecture contains two passive-control mechanisms, the "entrainment mechanism" and the "open-loop stable mechanism," that lead to the emergence of a self-organized temporal order in the whole system. This dynamic temporal pattern enables a robot to perform a stable rhythmic movement. We demonstrate a robot which juggles two balls rebounding off the wall and confirm the effectiveness of our approach.

KEYWORDS: Rhythm; Timing selection; Self-organization; Sensory-motor coordination; Passive control.

I. INTRODUCTION

Our goal is to realize natural motions with environmental adaptability in a simple robotic machine, based on biological principles of neuroscience, biology, psychology, and human behavior. This does not mean a mere mimicry of animal's apparent motion, but also an understanding of biological systems for engineering. Especially, we focus on the biomimetic control architecture, and consider the following questions: What is the key principle for adaptability to the environment? How can a robot adapt itself to a change in the environment? How should a robot be designed for dexterous motion? To solve these problems, there have been many attempts that aimed to establish a new information processing mechanism inspired by animal systems.[1]

In the life sciences, there is a view that the dynamics of life can be explained as a nonlinear phenomenon in a reaction-diffusion system. This view may be regarded as a fundamental principle of biomimetic robotics. Nature has many examples in which the synergy of local interactions generates a global order, such as the Southeast Asian synchronously flashing fireflies.[2] Spatial and temporal order in non-equilibrium physical and chemical systems can develop spontaneously. This self-organized pattern formation is a collective phenomenon and results from the interaction of a large number of subsystems.[3–5] Just as all systems in nature result from their interaction with surrounding systems, a robot should also exist through interaction with external systems. It is important to relate various movements caused by a non-equilibrium open system to adaptability to the environment.

A passive control, which exploits the dynamic system caused by the interaction between the environment and the body, is important from the viewpoint of achieving efficient control. Sensory-motor coordination using passive control has attracted attention and is being studied in the field of psychology and human science.[6] In biology, organisms have been considered to have nonlinear oscillators for many years,[5] and each neuron's mathematical model, including the rhythm bifurcations, is studied in detail in mathematical biology and neuroscience.[7,8] However, even if the response of each neuron is known, we may not be able to know the behavior of a neuron group, especially the whole behavior of neurons at the task level.

In robotics, the behavior at the task level is studied based on a more macroscopic viewpoint. Many robots using Central Pattern Generators (CPGs) have already been developed.[9–12] Williamson proposed a simple neural oscillator system coupled to a real robot arm, and demonstrated that, owing to the oscillators' entrainment, it is capable of coordinated motion without global synchronization or control.[10] His study is regarded as an application of Taga's idea[13,14] of global entrainment properties in human locomotion to a robot arm. His robot realized some rhythmic motions such as juggling. Juggling is one of the most interesting perceptual-motor tasks incorporating rhythmic movement, because the arm coordination generates various motion patterns of balls.

Based on the above background, this paper describes the architecture for rhythmic movement generation suited to a juggling-like task of "wall-bouncing," in which the robot repeats the process of bouncing two balls off the wall (Fig. 1). This is an example of a robotic task involving sensory-motor coordination. Our approach is similar to Williamson's approach in the "bidirectional coupling to the environment,"[15] which involves the effect of movement in both directions between the ball and the robot's arm. However, it is different in that our approach is "weak coupling to the environment," which does not require continuous monitoring of the environment, while Williamson's approach is "strong coupling".[15] Our approach, "bidirectional weak coupling,"[16–18] can adapt a robot to a change in the

* Dept. of Robotics, Ritsumeikan University, Kusatsu 525-8577, (Japan).
Corresponding author: E-mail: hirai-h@se.ritsumei.ac.jp
† Graduate School of Engineering Science, Osaka University, Toyonaka, Osaka 560-8531, Japan.

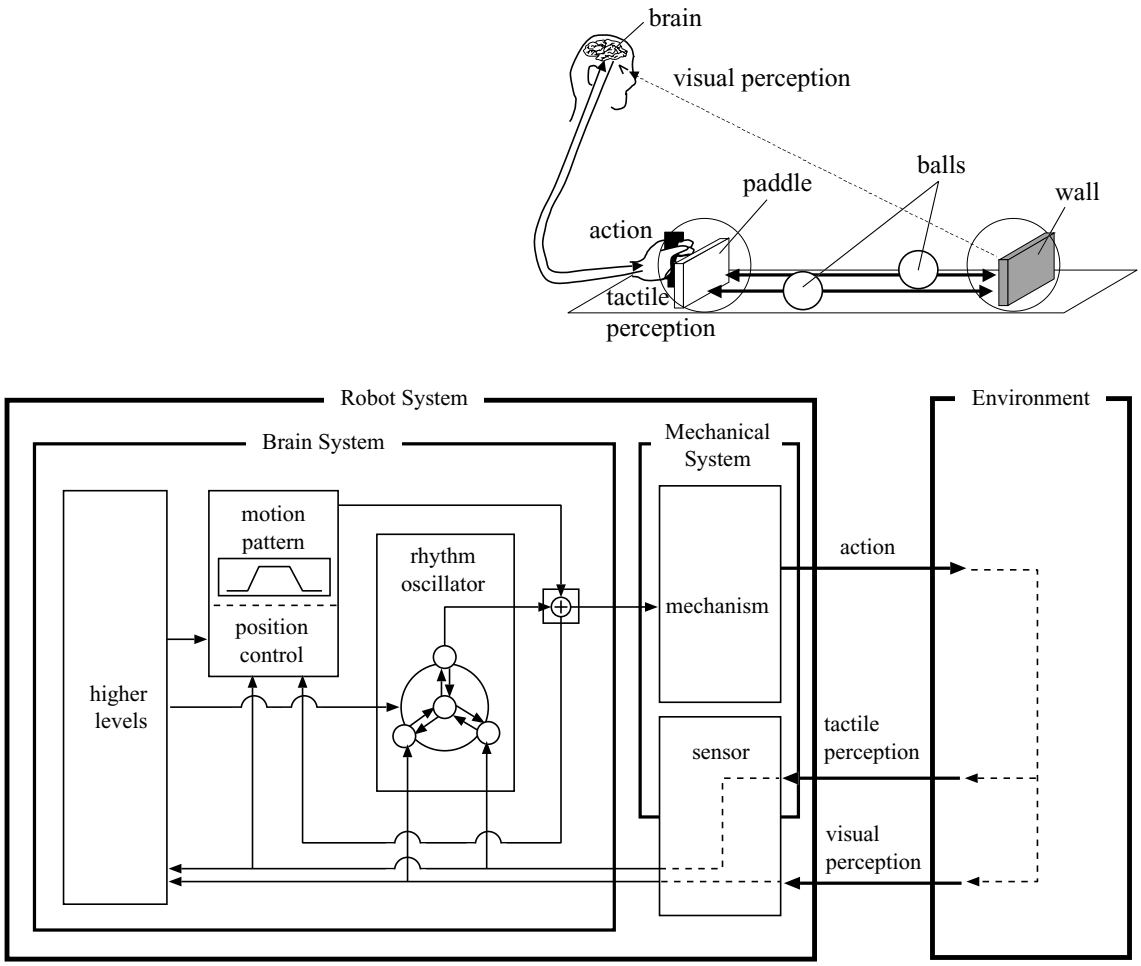

Fig. 1. Perceptual-motor system for robotic rhythm movement. The illustration shows a robot system that performs the wall-bouncing task. Both an action and two perceptions couple the robot with environment, and form the closed-loop system between the robot and the environment. The proposed Robot System consists of the Brain System and the Mechanical System. The Brain System is a hierarchical structure and it is divided into three sections: higher levels, a motion pattern and position control, and a rhythm oscillator. The Mechanical System is composed of a mechanism section and a sensor section.

environment, owing to the interaction between the robot and the environment at the ball contact.

In human behavior, Amazeen et al. studied the timing selection of rhythmic catching, and showed that humans control the timing of throwing and catching without the ball's entire flight information.[19] They showed the importance of timing information about the zenith of the ball's trajectory. Moreover, Sternad et al. reported that kinetic information about the impact is more necessary than visual information for rhythmic catching, although the latter gives information about the continuous kinetic trajectory of the ball.[20] Based on the above knowledge of human behavior, a touch sensor is attached to the robot's paddle and the wall. Only the time of the ball's contact with the paddle and the wall is the input to the robot. The timing of the paddle movement is adjusted by a proposed architecture for rhythmic movement generation. The robot recognizes the rhythm of the environment (balls) and adjusts the rhythm of the paddle movement to the balls' rhythm. This architecture contains a system of neural oscillators consisting of four weakly coupled Bonhöffer-van der Pol (BVP) oscillators to generate the appropriate timing of the paddle's movement. We call this system the bottom-up-fork-connected (BFC) robotic rhythm oscillator. The BFC robotic rhythm oscillator inputs touch-sensor information and outputs paddle-drive timing. This timing results from the self-organization (entrainment) of the whole system, including the internal and external environment, and is determined passively according to the dynamics of the whole system.

The proposed architecture consists of three redundant mechanisms, which are an active-control mechanism and two passive-control mechanisms. (Here, we use the words "passive control" to mean "not actively controlling.") The former mechanism is the "discrete feedback mechanism," and the latter mechanisms are the "open-loop stable mechanism" and the "entrainment mechanism." In this paper, we especially focus on two passive-control mechanisms. These mechanisms lead to the emergence of dynamic temporal pattern in the whole system. The coexistence and redundancy of these different mechanisms, which basically have an equivalent effect, guarantee faster recovery after a disturbance and make the whole system more stable.

This paper is structured as follows: In Section II, we propose a perceptual-motor system for robotic rhythmic

https://doi.org/10.1017/S0263574705002110 Published online by Cambridge University Press

movement, and present details of information processing within each section of a robot system. In Section III, we explain the two passive mechanisms of timing control, and show some simulation results to demonstrate the effectiveness of each mechanism. Later, we confirm the validity and effectiveness of our approach with both a human performance experiment (Section IV) and a robot experiment (Section V). Finally, in Section VI, we provide conclusions with some discussion.

II. ARCHITECTURE FOR RHYTHMIC MOVEMENT GENERATION

The proposed architecture for robotic rhythmic movement is outlined in Fig. 1. Both the action and perceptions of a robot couple the robot with the environment, and form the closed-loop system between the robot and the environment. This leads to a stable rhythmic motion in the whole system.

II.1. Brain system as sensory-motor pattern generator

II.1.1. Higher levels. Our robotic system is designed based on the hypothesis of a multilevel control system of movements. In this system, the higher levels determine the general characteristics of the task, such as *start*, *stop*, *continue*, and so on. These commands correspond to the value of a single parameter w explained in the section II.1.3.

II.1.2. Motion pattern and position control. Our system considers the pattern and timing of motion separately.

(2-a) Motion Pattern: The motion pattern is fixed. For example, it is a trapezoid pattern on the time vs. velocity map in Fig. 2. The paddle's velocity at the point of ball's impact is fixed as $V_p = 100$ mm/sec. The return velocity of the paddle, $-V_p'$, is also fixed at a certain value which ensures that the period of the paddle's movement is faster than that of the balls' movement, so that the paddle always hits the balls. The parameters τ_d and τ^n denote two moments of time relative to the time of the initial paddle movement. The former is the ideal timing of the ball's impact with the paddle, and the latter is the real timing of the nth ball's impact. The paddle is driven with the fixed motion pattern according to the timing calculated by other sections of the Brain System.

(2-b) Position Control: A robot needs to control the paddle's position specified in an external coordinate frame fixed to the ground. We adjust the timing calculated by the rhythm oscillator so as to achieve an ideal impact timing of τ_d at a specific impact position (Fig. 3). By shifting the timing of the initial paddle movement, we can discretely control the nth impact timing of τ^n.

Let the parameter t_p^n be the time of the nth initial paddle movement, the parameter t_b^n be the time of the nth ball's impact. After the nth ball's impact, the real impact timing τ^n is calculated as the difference between the time t_p^n and the time t_b^n. Then, the $n+1$th time regulation Δt_p^{n+1} is updated using the following rule:

$$\Delta t_p^{n+1} = \Delta t_p^n + \mathrm{sgn}(\tau_d - \tau^n)\Delta ts \tag{1}$$

where the ideal impact timing τ_d and a time step Δts are fixed as $\tau_d = 0.35$ seconds and $\Delta ts = 0.01$ seconds, respectively. The function sgn$(\cdot)$ denotes the signum function. This is the "active" control in an inertial coordinate frame.

II.1.3. Rhythm oscillator. The rhythm oscillator must adapt to the environment and conform to the higher-level commands in the Brain System. To solve this problem, we utilize the property of a neural oscillator (nonlinear oscillator) with a tonic input. Our proposed rhythm oscillator can adapt to the external condition "passively" and can also be ruled by higher-level commands, for example *start*, *stop*, and *continue*.

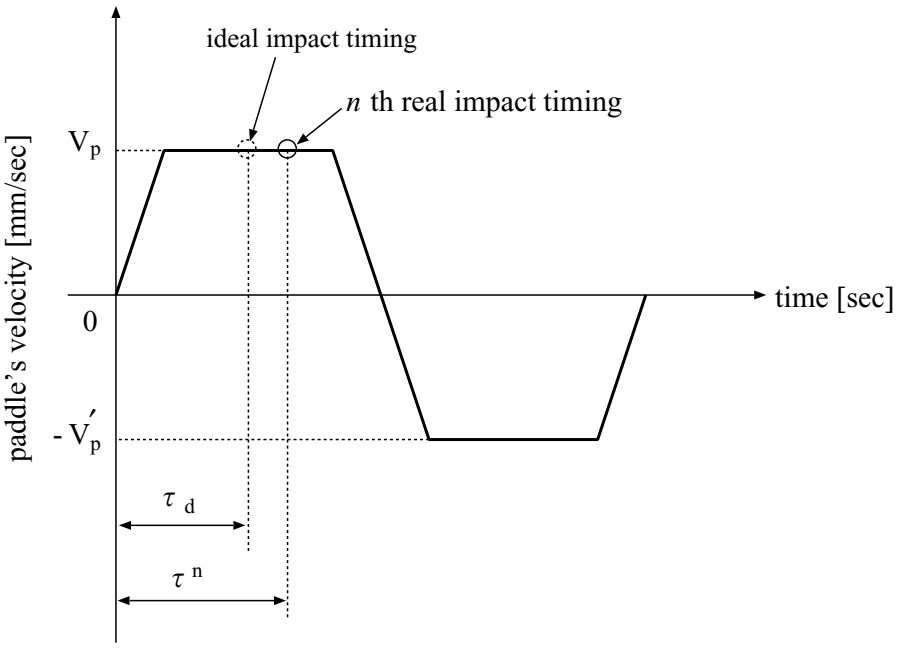

Fig. 2. Trapezoid pattern of paddle motion on time vs. velocity map. The paddle's velocity at the point of ball's impact, V_p, and the return velocity of the paddle, $-V_p'$, are fixed. The parameters τ_d and τ^n are, respectively, the ideal impact timing and the nth real impact timing.

https://doi.org/10.1017/S0263574705002110 Published online by Cambridge University Press

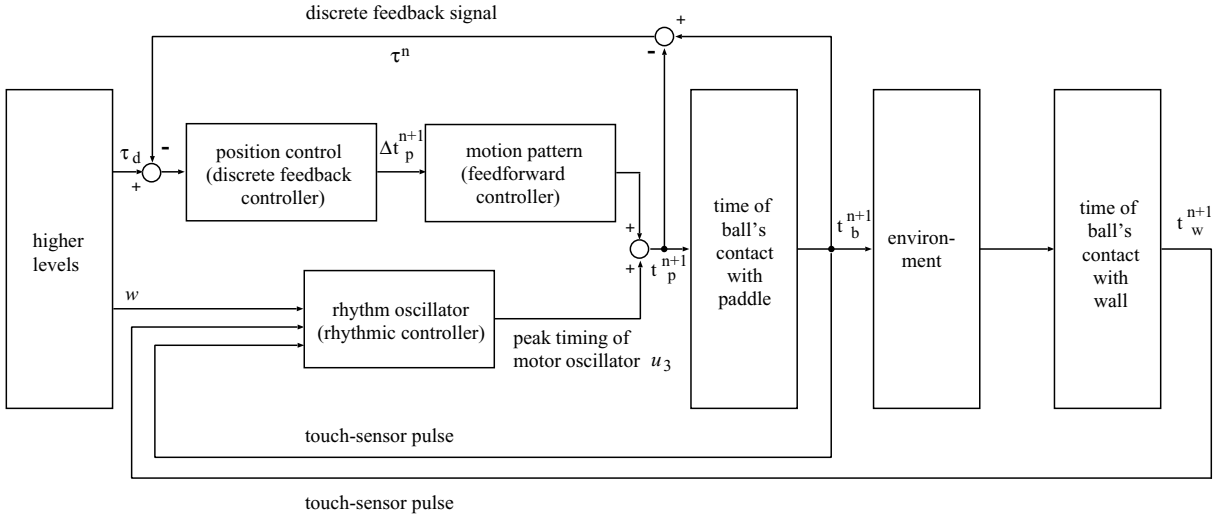

Fig. 3. Structure of timing control. The rhythm oscillator generates and adjusts the timing of the initial paddle movement according to three inputs: the tonic input w, and the two sensor pulses corresponding to the time of the ball's contact with the paddle and the wall. (t_b^{n+1} and t_w^{n+1} denote the moments of the time of the $n+1$th ball's contact with the paddle and the wall, respectively.) Moreover, the position control shifts by Δt_p^{n+1} the timing which is calculated by the rhythm oscillator, so as to achieve an ideal impact timing of τ_d at the specific impact position.

(3-a) Rhythm generation: We propose a system of neural oscillators consisting of four weakly coupled BVP oscillators named the bottom-up-fork-connected (BFC) robotic rhythm oscillator (Fig. 4). A BVP (or FitzHugh-Nagumo) oscillator is a simple neural model with two variables, and it is known that this model is the qualitative equivalent of the Hodgkin-Huxley neuron model which expresses the response of an actual neuron well. The proposed BFC robotic rhythm oscillator can be divided into three units: a sensor unit (osc1 and osc2); a rhythm unit (osc0); and a motor unit (osc3). Each sensor oscillator (osc1 and osc2) receiving sensor inputs is combined with a rhythm core oscillator (osc0), and information is transmitted synchronously. Similarly, the motor oscillator (osc3) outputting the timing of the paddle movement is mutually combined with a rhythm core oscillator (osc0). The rhythm core oscillator, which is the central unit of the BFC robotic rhythm oscillator, is not directly connected with the system's inputs and output. Sensor selection is easily adjusted by tuning coupling coefficients (δ_1 and δ_2). Which rhythm pattern emerges in a robot system closely relates to these coupling coefficients.

The model equation of each oscillator constituting the BFC robotic rhythm oscillator is given below:
Rhythm core oscillator (osc0):

$$\begin{cases} \frac{du_0}{dt} = \gamma_3\{v_0 + u_0 - \frac{1}{3}{u_0}^3 + \delta_1(u_1 - u_0) \\ \qquad\quad + \delta_2(u_2 - u_0) + \delta_3(u_3 - u_0) + w\} \\ \frac{dv_0}{dt} = -\frac{1}{\gamma_3}(u_0 + \gamma_2 v_0 - \gamma_1) \end{cases} \tag{2}$$

Sensor oscillator 1 (osc1):

$$\begin{cases} \frac{du_1}{dt} = \gamma_3\{v_1 + u_1 - \frac{1}{3}{u_1}^3 + \delta_1(u_0 - u_1) + w\} \\ \frac{dv_1}{dt} = -\frac{1}{\gamma_3}(u_1 + \gamma_2 v_1 - \gamma_1) \end{cases} \tag{3}$$

Sensor oscillator 2 (osc2):

$$\begin{cases} \frac{du_2}{dt} = \gamma_3\{v_2 + u_2 - \frac{1}{3}{u_2}^3 + \delta_2(u_0 - u_2) + w\} \\ \frac{dv_2}{dt} = -\frac{1}{\gamma_3}(u_2 + \gamma_2 v_2 - \gamma_1) \end{cases} \tag{4}$$

Motor oscillator (osc3):

$$\begin{cases} \frac{du_3}{dt} = \gamma_3\{v_3 + u_3 - \frac{1}{3}{u_3}^3 + \delta_3(u_0 - u_3) + w\} \\ \frac{dv_3}{dt} = -\frac{1}{\gamma_3}(u_3 + \gamma_2 v_3 - \gamma_1) \end{cases} \tag{5}$$

where the variable u_i $(i = 0, 1, 2, 3)$ represents the membrane potential of the neuron, and the parameter v_i $(i = 0, 1, 2, 3)$ represents the refractoriness. System parameters are fixed as $\gamma_1 = 0.7$, $\gamma_2 = 0.8$, and $\gamma_3 = 3.0$, because the behavior of a BVP oscillator using these parameters is analyzed well in the reference.[8] The coupling coefficient δ_1, δ_2, and δ_3 are tuned to generate the desirable pattern. The parameter w represents the current stimulation to the membrane model, and is controlled by the higher levels of the Brain System. If $w = 0.0$, the BFC robotic rhythm oscillator does not fire, even if the sensor pulse is added to a robot. This parameter value $w = 0$ corresponds to the higher-level command *stop*. When the parameter w is decreased, the BFC robotic rhythm oscillator is activated according to the sensor input. Then, the value of the parameter w corresponds to the higher-level command *start* or *continue*. Note that a negative input represents an excitation stimulus in this BVP oscillator model. This parameter w is also tuned according to the desirable output pattern. (We fixed $w = -0.05$ or -0.2 as a tonic input in the following task.) We assume the duty cycle of stimulation pulse to be zero. That is, a sensor pulse instantaneously shifts the membrane potential u_i to $u_i - 1.0$ $(i = 1, 2)$, when sensor signal inputs to a sensor oscillator (osc1 or osc2). In addition, referring to bifurcation diagrams of a (not connected) BVP oscillator stimulated

https://doi.org/10.1017/S0263574705002110 Published online by Cambridge University Press

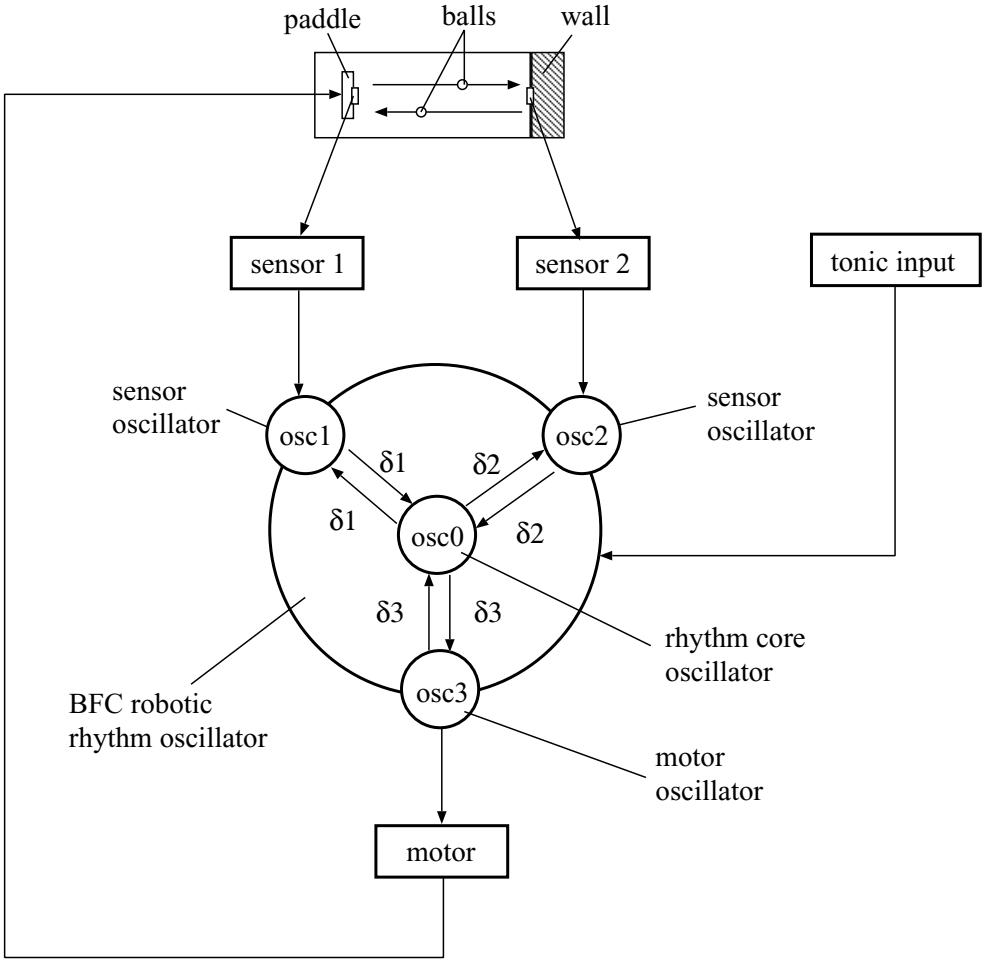

Fig. 4. General concept of the BFC robotic rhythm oscillator. The BFC robotic rhythm oscillator is a system of neural oscillators consisting of four weakly coupled BVP oscillators. The BFC robotic rhythm oscillator can be divided into three kinds of oscillators: a sensor oscillator (osc1 and osc2) receiving sensor inputs; a rhythm core oscillator (osc0) which is the central unit of the BFC robotic rhythm oscillator; and a motor oscillator (osc3) outputting the timing of the paddle movement. Three marginal oscillators (osc1, osc2, and osc3) are mutually combined with the rhythm core oscillator (osc0) respectively, and information is transmitted synchronously. The parameters δ_1, δ_2 and δ_3 denote coupling coefficients between each marginal oscillator and the rhythm core oscillator. The BFC robotic rhythm oscillator can adapt to sensor inputs and can also be ruled by tonic input.

by periodic pulse trains,[8] we adopted different time scales between the rhythm oscillator and the real world, that is, 60:1, so that the time scale of the response of the rhythm oscillator corresponds to the time scale of a cycle in the task. All the numerical computations were carried out in double precision, using a fourth order Runge-Kutta method and the time step $\Delta t = 0.01$ seconds.

Figures 5 and 6 show the responses of the BFC robotic rhythm oscillator to a single impulsive input in two cases: the case (a) in which all oscillators are connected mutually by reciprocal inhibition ($\delta_1 = \delta_2 = \delta_3 = 0.1$, $w = -0.2$), and the case (b) in which the rhythm core oscillator (osc0), the sensor oscillator 1 (osc1), and the motor oscillator (osc3) are connected by reciprocal inhibition but the rhythm core oscillator (osc0) and the sensor oscillator 2 (osc2) are connected by reciprocal excitation ($\delta_1 = \delta_3 = 0.1$, $\delta_2 = -0.1$, $w = -0.05$). (Note that the direction of the vertical axis of the graphs, which illustrate the membrane potentials of each oscillator, is opposite to the conventional direction. We intentionally place negative values above zero, so that the excitation is upward.) The left graphs in Figs 5 and 6, which are indexed as (a-1) and (b-1), respectively, show the responses of each oscillator in the case that a single impulsive input is added to the sensor oscillator 1 (osc1), while the right graphs in Figs 5 and 6, which are indexed as (a-2) and (b-2), respectively, display the responses of each oscillator in the case of a single impulsive input to the sensor oscillator 2 (osc2). In both cases (a-1) and (a-2), because each sensor oscillator (osc1, osc2) is coupled to the rhythm core oscillator (osc0) symmetrically, the stimulus to each sensor oscillator influences the rhythm core oscillator similarly. Moreover, these effects diffuse from the rhythm core oscillator (osc0) to the motor oscillator (osc3). Thus, all four oscillators tend to synchronize through the diffusive couplings. In Fig. 5, the sensor oscillator without the impulsive input and the motor oscillator (osc3) mutually synchronize in phase. On the other hand, in case (b), two response patterns exist according to which sensor oscillator is stimulated, because two sensor oscillators are connected to the rhythm core oscillator asymmetrically. If a single impulse is added to the sensor oscillator 1 (osc1), the motor oscillator (osc3) synchronizing with other oscillators fires with a slight time

https://doi.org/10.1017/S0263574705002110 Published online by Cambridge University Press

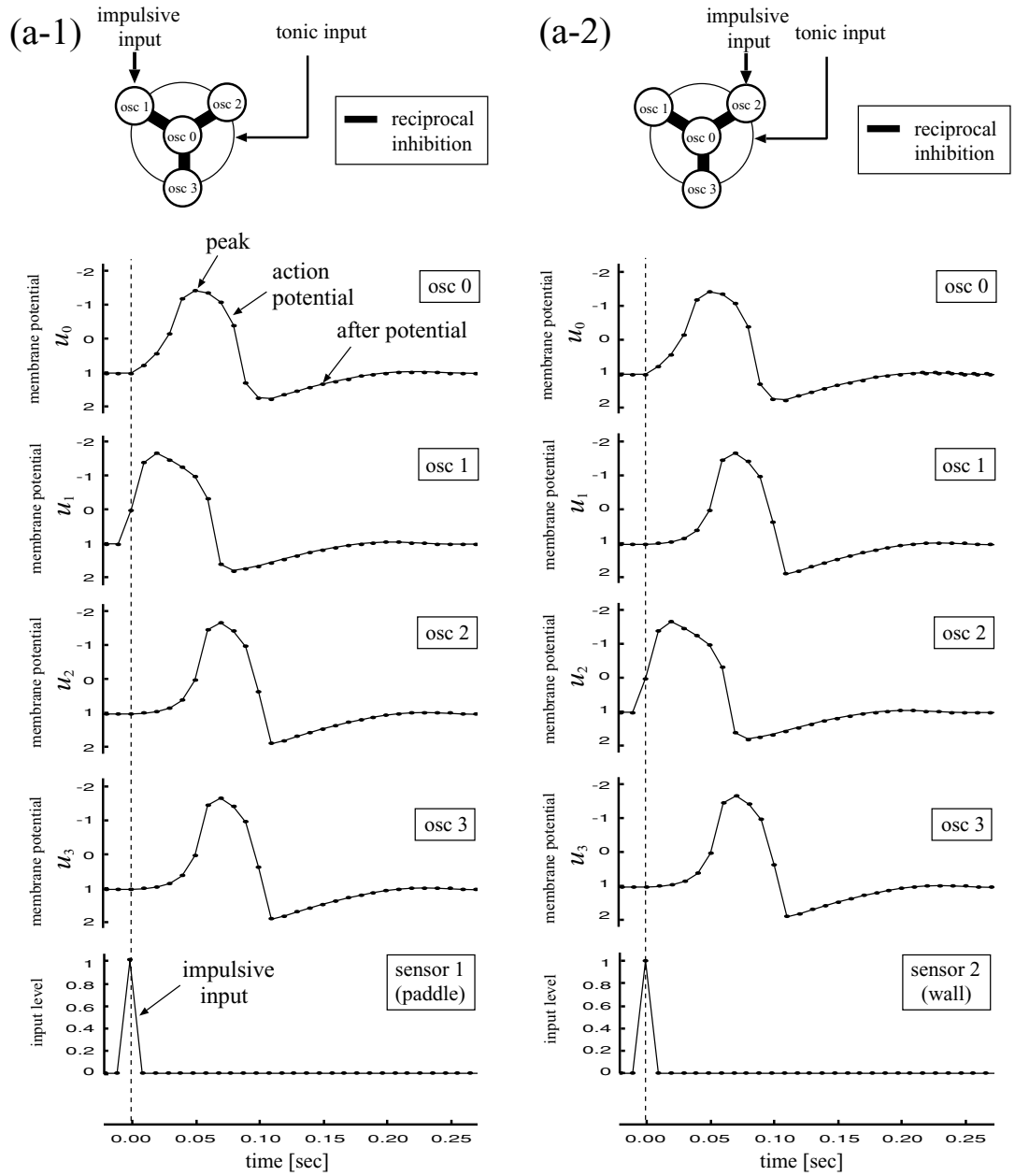

Fig. 5. Response of BFC robotic rhythm oscillator to single impulsive input ($\delta_1,\ \delta_2,\ \delta_3 = 0.1, w = -0.2$): all marginal oscillators are connected to the rhythm core oscillator by reciprocal inhibition. (a-1) a single impulsive input to the sensor oscillator 1; and (a-2) a single impulsive input to the sensor oscillator 2.

delay (Fig. 6 (b-1)). However, even if the stimulus is added to the sensor oscillator 2 (osc2), the motor oscillator 3 (osc3) does not fire (Fig. 6 (b-2)). This stimulus causes the rhythm core oscillator (osc0) to go out of phase, thus playing the role of the upbeat. (The upbeat is an unaccented rhythm beat preceding an accented rhythm beat.)

(3-b) Compensation for phase difference: In forced synchronization, the phases of an external signal and an oscillator cannot be locked in general, although their frequencies can be synchronized by frequency entrainment. To tune these phases, the position control in Section II.1.2 roughly shifts the timing calculated by the rhythm oscillator. As shown in Fig. 3, the time shift for phase compensation is realized in both the discrete feedback control and the rhythmic control, and the time of the initial paddle movement is described by the following equation:

$$t_p^{n+1} = t_p^n + \Delta t_p^{n+1} + [\text{contribution of BFC robotic rhythm oscillator's output}] \quad (6)$$

The rhythm oscillator changes the time interval dynamically, while the discrete feedback adjusts the timing step by step. The task is performed successfully by the synergy of these effects.

II.2. Mechanical system

II.2.1. Sensor. The touch sensors are attached to the robot's paddle and the wall. These sensors have different roles: the touch sensor on the robot's paddle is the timing receptor as

https://doi.org/10.1017/S0263574705002110 Published online by Cambridge University Press

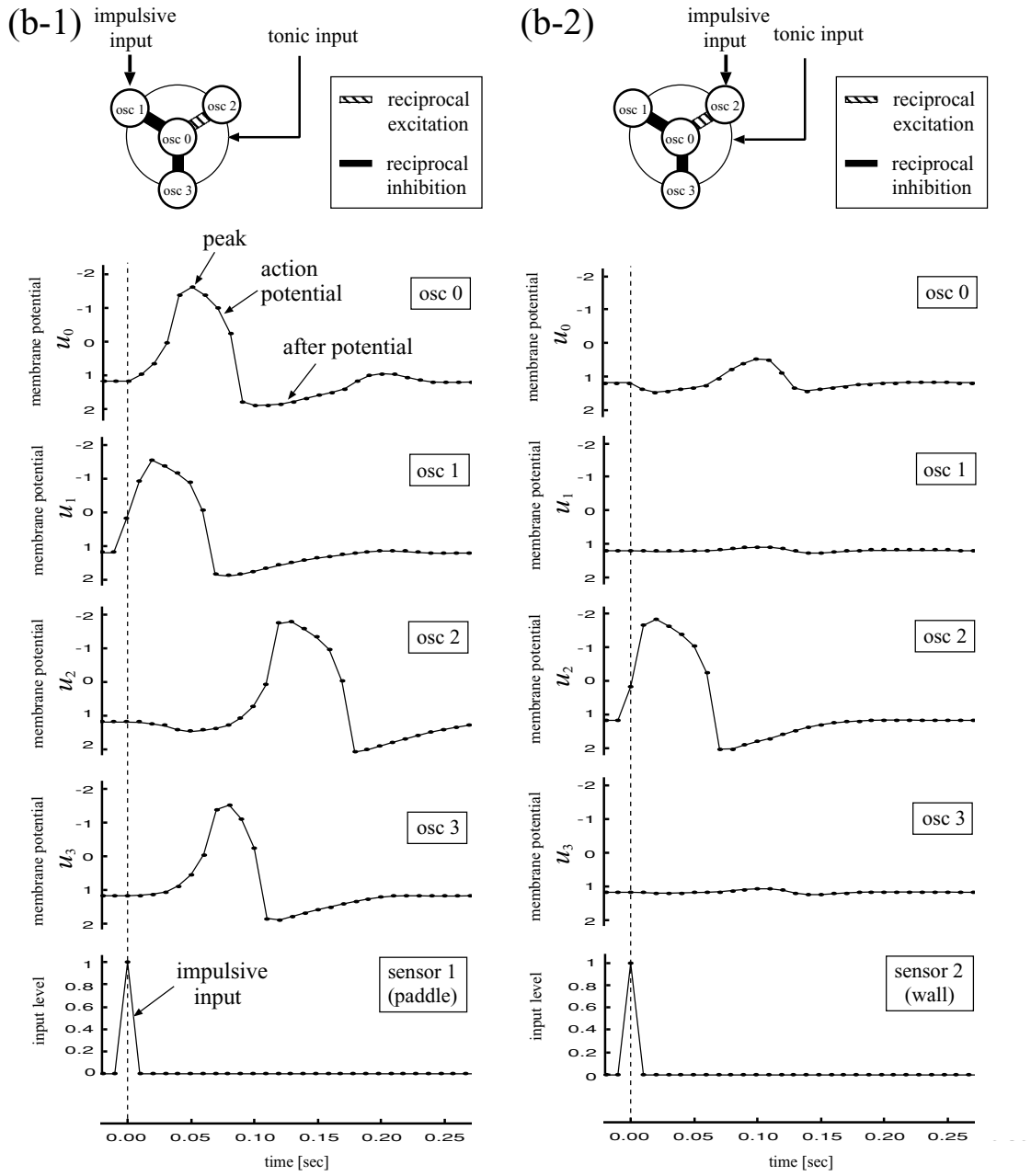

Fig. 6. Response of BFC robotic rhythm oscillator to single impulsive input ($\delta_1,\ \delta_3 = 0.1,\ \delta_2 = -0.1,\ w = -0.05$): the sensor oscillator 1 (osc1) and the motor oscillator (osc3) are connected to the rhythm core oscillator (osc0) by reciprocal inhibition, but the sensor oscillator 2 (osc2) is connected to the rhythm core oscillator (osc0) by reciprocal excitation. (b-1), a single impulsive input to the sensor oscillator 1; and (b-2) a single impulsive input to the sensor oscillator 2.

a substitute for the player's tactile sensor, while the touch sensor on the wall is the timing receptor as a substitute for the player's visual sensor (Fig. 1). Only the time stamp of a ball contacting the paddle and the wall is input into the robot.

II.2.2. Mechanism. One straightforward viewpoint about structure of motor program is the "impulse-timing hypothesis".[21] The motor program provides pulses of motor neuron activity to the relevant musculature. These pulses produce patterns of contractions in the muscles. The major role of motor program is to "tell" the muscles when to turn on, how much force to use, and when to turn off. In our robot system, the Brain System, which calculates the appropriate timing of movement, tells the motor of the paddle when to move and the paddle is driven with the predetermined motion pattern.

III. PASSIVE MECHANISMS OF TIMING CONTROL

The architecture proposed in Section II consists of an active-control mechanism and two passive-control mechanisms (Fig. 7). The "discrete feedback mechanism" works as an active control in our architecture. A robot adjusts the internal timing of the paddle movement with the intention of keeping an ideal impact point, based on the discrete timing information about a ball contacting the paddle. This mechanism is correspond to the system proposed in Section II.1.2

https://doi.org/10.1017/S0263574705002110 Published online by Cambridge University Press

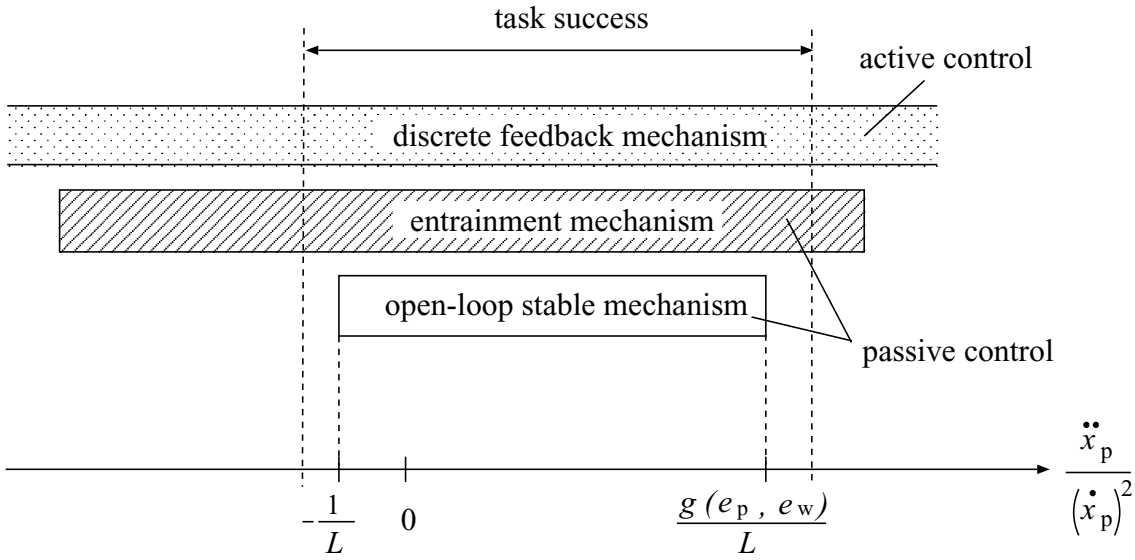

Fig. 7. Three redundant mechanisms of timing control: (1) the discrete feedback mechanism, which is realized by position control; (2) the entrainment mechanism, which is realized by the BFC robotic rhythm oscillator; and (3) the open-loop stable mechanism, which is related to the operation parameter $\ddot{x}_p/(\dot{x}_p)^2$ on the horizontal axis. This illustration also shows the range of open-loop stability. (Please refer to Section III.1 for details.) The discrete feedback mechanism works as an active control, while the entrainment mechanism and the open-loop stable mechanism work as passive controls. The synergy of these three mechanisms leads to the stable performance of the successful wall-bouncing task.

(2-b). It requires absolute information such as the parameter τ_d, and is capable of adjusting the timing of the robot's motion to the timing of the environment (ball). (Refer to the reference [18] for more information about the active control in our architecture.) On the other hand, both the "open-loop stable mechanism" and the "entrainment mechanism" work as passive controls. The "open-loop stable mechanism" is closely related to the paddle's motion pattern mentioned in Section II.1.2 (2-a), and it is capable of adjusting the environment, that is the ball's motion, so as to keep the robot's motion stable. The "entrainment mechanism" is realized by the rhythm oscillator proposed in Section II.1.3, and it is capable of adapting the robot's motion to the environment. This mechanism requires relative information, and a robot generates and adjusts the timing of the paddle movement so as to keep the timing of the ball's contact with the paddle same as the one at the last impact. These three mechanisms are redundant and they basically produce an equivalent effect. The synergy of these different mechanisms leads to the stable performance of the successful task. In this paper, we especially focus on two passive-control mechanisms, the "open-loop stable mechanism" and the "entrainment mechanism." These passive-control mechanisms guarantee the dynamic stability of the whole system in the wall-bouncing-juggling task. We propose a passive-control strategy exploiting these mechanisms. However, an active control, such as a feedback control, also contributes to the stability of the system. We consider that the passive-control strategy using the dynamic stability of the system is more powerful and significant than an elaborate feedback control strategy and we believe that humans must exploit the passive-control strategy from the result of the human performance experiment in the following Section IV.

III.1. Open-loop stable mechanism

The wall-bouncing task is the repeated action of hitting a ball against a wall. The ball rolls or slides on a horizontal plane and rebounds off a wall (Fig. 8). Although this task seems to be simple, modeling its physical phenomenon is not easy. We discuss the open-loop stability of the system using a model obtained on the following assumptions: (1) the ball is a particle mass, (2) no friction acts between the ball and the plane, and (3) the paddle is periodically driven with a fixed motion pattern at a constant frequency. In this section, we deal with only the open-loop stable mechanism, and use neither the entrainment mechanism nor the discrete feedback mechanism to control the ball. Table I shows the relationship between three timing-control mechanisms used in the following simulation experiments.

III.1.1. Local linear stability. Let the variable t_n be the interval between the nth impact and $n+1$th impact, the variables x_b^n, $\dot{x}_b^n$, x_p^n, $\dot{x}_p^n$ be, respectively, the horizontal positions and velocities of the ball and the paddle immediately before the nth impact, e_p, e_w be, respectively, coefficients of restitution of the paddle and the wall. Then, the motion of the ball is expressed as a discrete system:

$$x_b^{n+1} = x_p^{n+1} \tag{7}$$

$$\dot{x}_b^{n+1} = e_w e_p \dot{x}_b^n - e_w(1+e_p)\dot{x}_p^n \tag{8}$$

If we describe an equilibrium point of this discrete system as $(x_b, \dot{x}_b) = (X_b, V_b)$, the distance between the paddle and the wall, L, is written as

$$L = L_w - X_b \tag{9}$$

https://doi.org/10.1017/S0263574705002110 Published online by Cambridge University Press

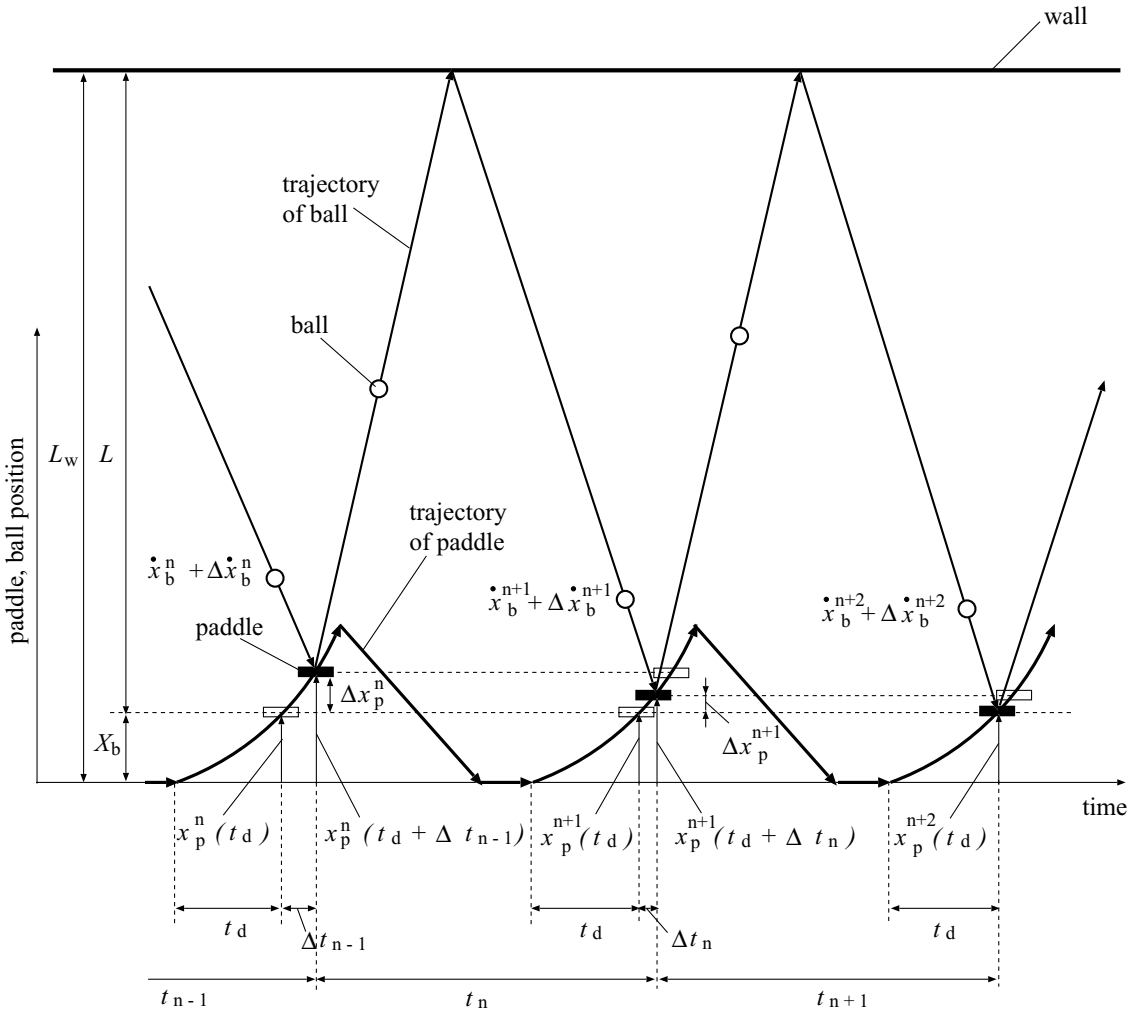

Fig. 8. Model of the wall-bouncing task with perturbation. The wall-bouncing task is the repeated action of hitting a ball against a wall. The paddle is driven with a fixed motion pattern at the constant frequency. After the paddle hits the ball, the ball rolls on a horizontal plane and rebounds off the wall. The position and velocity of the ball at the nth impact affects the states of the ball at the following impacts.

where L_w is the position of the wall. Then, the interval of consecutive impacts t_d is given by

$$t_d = \frac{L}{(1+e_p)V_p - e_p V_b} + \frac{L}{e_w\{(1+e_p)V_p - e_p V_b\}} \quad (10)$$

where V_p is the constant paddle velocity at impact. Considering the finite increment $\mathbf{\Delta} = (\Delta t_n, \Delta x_b^n, \Delta \dot{x}_b^n, \Delta x_p^n, \Delta \dot{x}_p^n)$ from an equilibrium point, we can obtain the following equation of the ball's motion by linearizing the above equations about the equilibrium point.

$$\mathbf{\Delta x}_b^{n+1} = \boldsymbol{P} \cdot \mathbf{\Delta x}_b^n \quad (11)$$

$$\mathbf{\Delta x}_b^n = \begin{pmatrix} \Delta x_b^n \\ \Delta \dot{x}_b^n \end{pmatrix}$$

$$\boldsymbol{P} = \begin{pmatrix} f_1(e_p, e_w, L, \dot{x}_p, \ddot{x}_p) & f_2(e_p, e_w, L, \dot{x}_p, \ddot{x}_p) \\ f_3(e_p, e_w, \dot{x}_p, \ddot{x}_p) & f_4(e_p, e_w) \end{pmatrix}$$

Table I. Relationship between simulation experiments and the three timing-control mechanisms.

	Passive control		Active control
Simulation experiment	Open-loop stable mechanism	Entrainment mechanism	Discrete feedback mechanism
ex.1(a) (Section III.1, Fig. 9(a))	nonuse	nonuse	nonuse
ex.1(b) (Section III.1, Fig. 9(b))	use	nonuse	nonuse
ex.2(a) (Section III.2, Fig. 10(a))	nonuse	use	nonuse
ex.2(b) (Section III.2, Fig. 10(b))	use	use	nonuse
ex.3 (Section III.2, Fig. 11)	use	use	use

https://doi.org/10.1017/S0263574705002110 Published online by Cambridge University Press

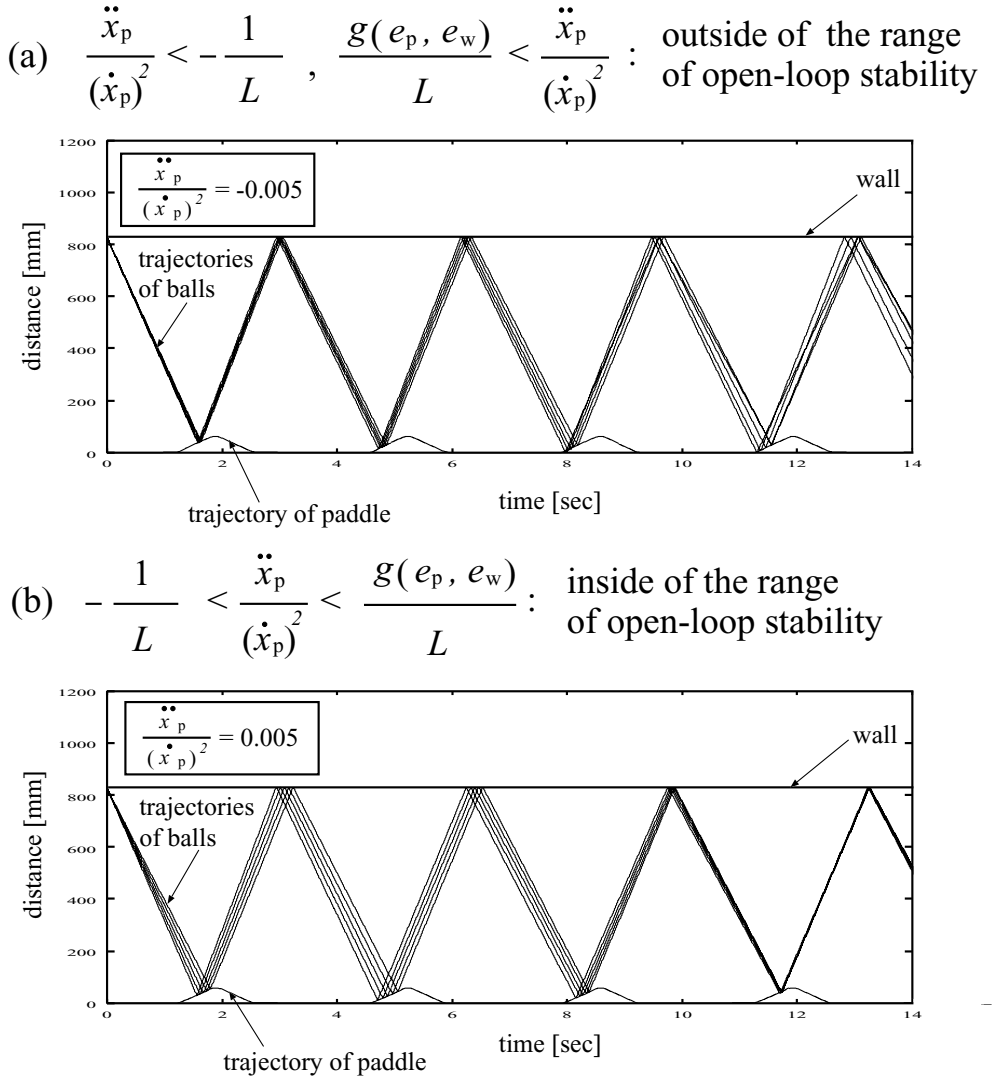

Fig. 9. Influences of the paddle's movement on open-loop stability (ex.1). In this simulation, the range of open-loop stability is $-0.0013 < \ddot{x}_p/(\dot{x}_p)^2 < 0.0056$. (a) If the operation parameter $\ddot{x}_p/(\dot{x}_p)^2$ is out of range, $\ddot{x}_p/(\dot{x}_p)^2 = -0.005$, the ball's trajectories diverge with time; (b) if the operation parameter is within the range, $\ddot{x}_p/(\dot{x}_p)^2 = 0.005$, the ball's trajectories converge with time.

where f_1, f_2, f_2 and f_4 are certain nonlinear functions. Then, at least under the condition $e_w, e_p > 0.543$, the condition for local linear stability is written in the following form:

$$-\frac{1}{L} < \frac{\ddot{x}_p}{(\dot{x}_p)^2} < \frac{g(e_p, e_w)}{L} \tag{12}$$

where $g(e_p, e_w)$ is

$$g(e_p, e_w) = \frac{2e_w(1+e_p)}{(1+e_w)(1-e_p e_w)} \tag{13}$$

Note that the nonlinear functions $g(e_p, e_w)$ are always positive. Equation (12) means that an operation parameter $\ddot{x}_p/(\dot{x}_p)^2$ has to be within a certain range defined as an inequality of environmental parameters. This range corresponds to the domain of the open-loop stability in Fig. 7. Figure 9 shows that the stability of ball's motion is influenced by the paddle's movement at the point of ball's impact. Some balls start at the same position but with slightly different initial velocity condition, and the robot hits each ball with a fixed motion pattern. In this simulation, we fixed the parameters as $L = 800$ mm, $e_w = e_p = 0.8$, respectively. Substituting these values into Equation (12), we can obtain the following condition for open-loop stability:

$$-0.0013 < \frac{\ddot{x}_p}{(\dot{x}_p)^2} < 0.0056 \tag{14}$$

If the operation parameter is out of range, $\ddot{x}_p/(\dot{x}_p)^2 = -0.005$, the ball's trajectories diverge with time (Fig. 9(a)). In this case, the other control is necessary to achieve stability in the system. Otherwise, the robot fails to hit a ball after several ball's impacts. On the other hand, if this operation parameter $\ddot{x}_p/(\dot{x}_p)^2$ is within the range of Equation (14), $\ddot{x}_p/(\dot{x}_p)^2 = 0.005$, the motion of a ball is stable owing to the open-loop stability, and the ball's trajectories converge with time (Fig. 9(b)). In the case that we cannot know environmental parameters, if the paddle is driven at the impact with $\ddot{x}_p = 0$, that is with a constant velocity, the motion of the ball is stabilized passively because $\ddot{x}_p = 0$

https://doi.org/10.1017/S0263574705002110 Published online by Cambridge University Press

always satisfies Equation (12). This is a most interesting result of the local stability analysis. In Section IV, we confirm by the human movement experiment that humans may exploit this condition for the stable control of a ball. This result corresponds to the hypothesis shown by Sternad et al. in the one-handed ball bouncing task.[20]

III.1.2. Global stability. In the special case that the following two conditions are satisfied: (1) the paddle is driven with a fixed velocity V_p at the impact, and (2) the impact position is fixed, we can also prove the global stability of the system. Because the former condition always satisfies Equation (12), the local stability is naturally guaranteed. Considering Equation (8) as the one-dimensional map $h(\dot{x}_b^n, V_p)$, it is possible to define the subsequent sequence $\{\dot{x}_b^n\}$:

$$\dot{x}_b^n = h\left(\dot{x}_b^{n-1}, V_p\right) = h^2\left(\dot{x}_b^{n-2}, V_p\right) = \cdots = h^{n-1}\left(\dot{x}_b^1, V_p\right) \tag{15}$$

Then, the velocity of a ball at the nth impact $\dot{x}_b^n$ is expressed as the following equation:

$$\dot{x}_b^n = (e_w e_p)^{n-1}\dot{x}_b^1 - \frac{e_w(1+e_p)V_p}{1-e_w e_p}\left(1-(e_w e_p)^{n-1}\right) \tag{16}$$

where $\dot{x}_b^1$ is the initial velocity of a ball. Coefficients of restitution of the paddle and the wall e_p, e_w always satisfy $|e_p| < 1$ and $|e_w| < 1$. Therefore, for any initial velocities $\dot{x}_b^1$, the subsequent sequence $\{\dot{x}_b^n\}$ converges at a certain value V_b:

$$V_b = \lim_{n\to\infty} \dot{x}_b^n = -\frac{e_w(1+e_p)V_p}{1-e_w e_p} \tag{17}$$

Similarly, we can prove the global stability of the system under more general conditions considering the effects of gravity, friction and ball rotation. Then, the subsequent sequence $\{\dot{x}_b^n\}$ is expressed as the following equations:

$$\dot{x}_b^1 \le 0 \tag{18}$$

$$\dot{x}_b^{n+1} = -\sqrt{\left(a\dot{x}_b^n + b\right)^2 + c} \tag{19}$$

$$(-1 < a < 0,\ b > 0,\ c > 0)$$

where a, b, c are nonlinear functions of e_p, e_w, V_p, and so on. (Refer to Appendix for details.) The subsequent sequence $\{\dot{x}_b^n\}$ is interpreted as the points on the Poincaré section $\Sigma = \{\{\dot{x}_b^n\} \in \boldsymbol{R}^1 | n \in \boldsymbol{N}, x_b^n = x_p^n\}$, and Equation (19) is the Poincaré map. The convergence of the ball's motion can be derived by replacing the problem of the continuous ball's motion with the problem of the discrete mapping on the Poincaré section Σ. We can prove mathematically that the subsequent sequence $\{\dot{x}_b^n\}$ converges from all initial states, as shown in the Appendix. Therefore, the convergence of the ball's continuous motion is guaranteed. These results show that if the position and the velocity of the paddle can be fixed at the point of impact, the motion of the ball is stabilized for all initial conditions and all slope angles. Once the motion of the ball is stabilized around the equilibrium point, the position and the velocity of the ball are kept stable by local stability. Therefore, the robot should choose the following strategy for open-loop stability: "Hit the ball with a fixed velocity at a fixed position." To apply this strategy, we propose the architecture using the BFC robotic rhythm oscillator. In the next section III.2, we demonstrate some simulation experiments using the BFC robotic rhythm oscillator, and describe the effect of the entrainment mechanism.

III.2. Entrainment mechanism

To confirm the effectilveness of the entrainment mechanism in our robot system, we simulated the wall-bouncing task with two balls. The wall-bouncing robot repeats the process of hitting two balls rebounding off the wall with a fixed motion pattern. The two horizontal guide rails are arranged parallel to each other, and each ball is always rolling on a separate guide. For the sake of simplicity, we assume that each ball is a particle mass and no friction acts between the ball and the plane. The initial velocities of balls are 500 mm/sec and 600 mm/sec. The system is perturbed through random changes in the coefficients of restitution between the ball and the paddle or the wall. The pseudo-random number generator generates the coefficients varying at random between 0.80 to 0.82. The distance between the robot and the wall is 800 mm. The touch sensors are attached to the robot's paddle and the wall, and only the time of the ball's contact with the paddle or the wall is detectable, while the robot cannot distinguish one ball from the other. In this simulation, we fixed the coupling coefficient parameters of the BFC robotic rhythm oscillator as $\delta_1 = \delta_2 = \delta_3 = 0.1$. The tonic input parameter was also fixed as $w = -0.2$.

Figure 10 shows the simulation results in two cases: the case (a) in which only the entrainment mechanism is used and other mechanisms are not used, and the case (b) in which both the open-loop stable mechanism and the entrainment mechanism are used and the discrete feedback mechanism is not used. (Refer to ex.2 (a) and (b) in Table I.) In case (a), if the entrainment mechanism does not work, the balls' trajectories should diverge with time because the operation parameter $\ddot{x}_p/(\dot{x}_p)^2$ is out of the range of Equation (12). However, owing to the entrainment mechanism of the BFC robotic rhythm oscillator, the robot adjusts the timing of the initial paddle movement and struggles to keep hitting two balls, although each ball's impact point is still scattered. In case (b), both the entrainment mechanism and the open-loop stable mechanism work for the balls' timing control and the synergy of these mechanisms realizes the stable hitting of two balls. Then, the interval of time between balls' impacts are kept almost equal because the BFC robotic rhythm oscillator locks two timings of the ball's contact with the paddle and the wall in phase and because the open-loop mechanism stabilizes the balls' trajectories.

Moreover, to show the environmental adaptability of our architecture, we changed the distance between the robot and the wall, L, from 800 mm to 1100 mm. A change in the distance between the robot and the wall leads to a change in the timing of hitting. In this simulation, we used all three mechanisms, which are the open-loop stable mechanism, the entrainment mechanism and the discrete feedback mechanism. (Refer to ex.3 in Table I.) The paddle is driven

https://doi.org/10.1017/S0263574705002110 Published online by Cambridge University Press

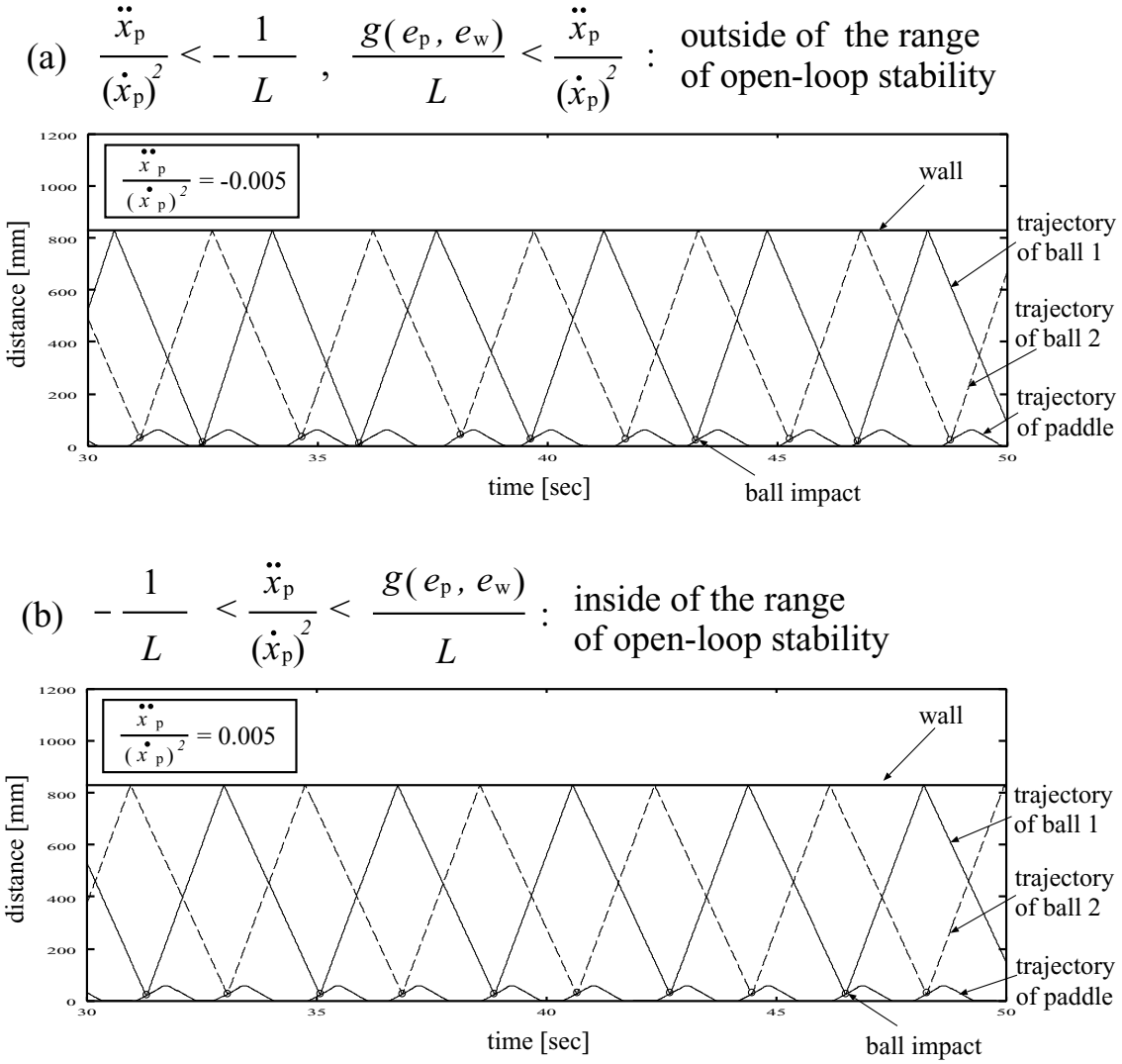

Fig. 10. Effect of entrainment in the wall-bouncing task (ex.2). In (a), only the entrainment mechanism is used. The robot adjusts the timing of the initial paddle movement and struggles to keep hitting two balls, although each ball's impact point is scattered. In (b), both the open-loop stable mechanism and the entrainment mechanism are used. The interval of time between balls' impacts are kept almost equal because the BFC robotic rhythm oscillator locks two timings of the ball's contact with the paddle and the wall in phase and because the open-loop mechanism stabilizes the balls' trajectories.

with a constant velocity at the point of contact with the balls so that the open-loop stable mechanism always works independently of the distance parameter L . The other conditions of the simulation are the same as the ones in the wall-bouncing task with two balls (ex.2). Figure 11 shows two kinds of trajectories, the paddle's trajectory and the two balls' trajectories. The lower graphs (c-1) and (c-2) in Fig. 11 is the enlargement of the regions (1) and (2) in the top graph (a) in Fig. 11. A robot changes the time interval of hitting according to a change in the environment, owing to the following effects: (1) the self-organized timing selection by frequency entrainment of the BFC robotic rhythm oscillator and (2) the appropriate timing shift by the discrete feedback mechanism. The BFC robotic rhythm oscillator settles down in a certain fixed behavioral attractor. A robot keeps hitting two balls at an almost equal interval of time, owing to the phase-lock effect of the BFC robotic rhythm oscillator. Moreover, the open-loop stable mechanism contributes to achieving the stable ball's impact by adjusting the balls' motion. To realize the same effect using only feedback control, an elaborate complex strategy was required. We also changed the tonic input w from $w = -0.2$ to 0.0 at 900.0 seconds as a higher-level command of the Brain System, *stop*. The robot stops the paddle, obeying this command. (Note again that in graph (b) in Fig. 11, the direction of the vertical axis is opposite to the custom direction so that the excitation stimulus is upward.)

Our approach is interpreted as "bidirectional coupling to the environment",[16–18] because this approach involves the effects of both directions between the ball and the paddle, and is also interpreted as "weak coupling to the environment",[16–18] because this approach requires only the discrete information about the ball's impact. Moreover, our approach is categorized as belonging to the class of feedforward control (and the discrete feedback control) in contrast with the traditional feedback-based approach,[22] which requires continuously monitoring the environment (i.e. strong coupling). Our robot, which relies on minimal sensing and small processors, is relatively simple compared with

https://doi.org/10.1017/S0263574705002110 Published online by Cambridge University Press

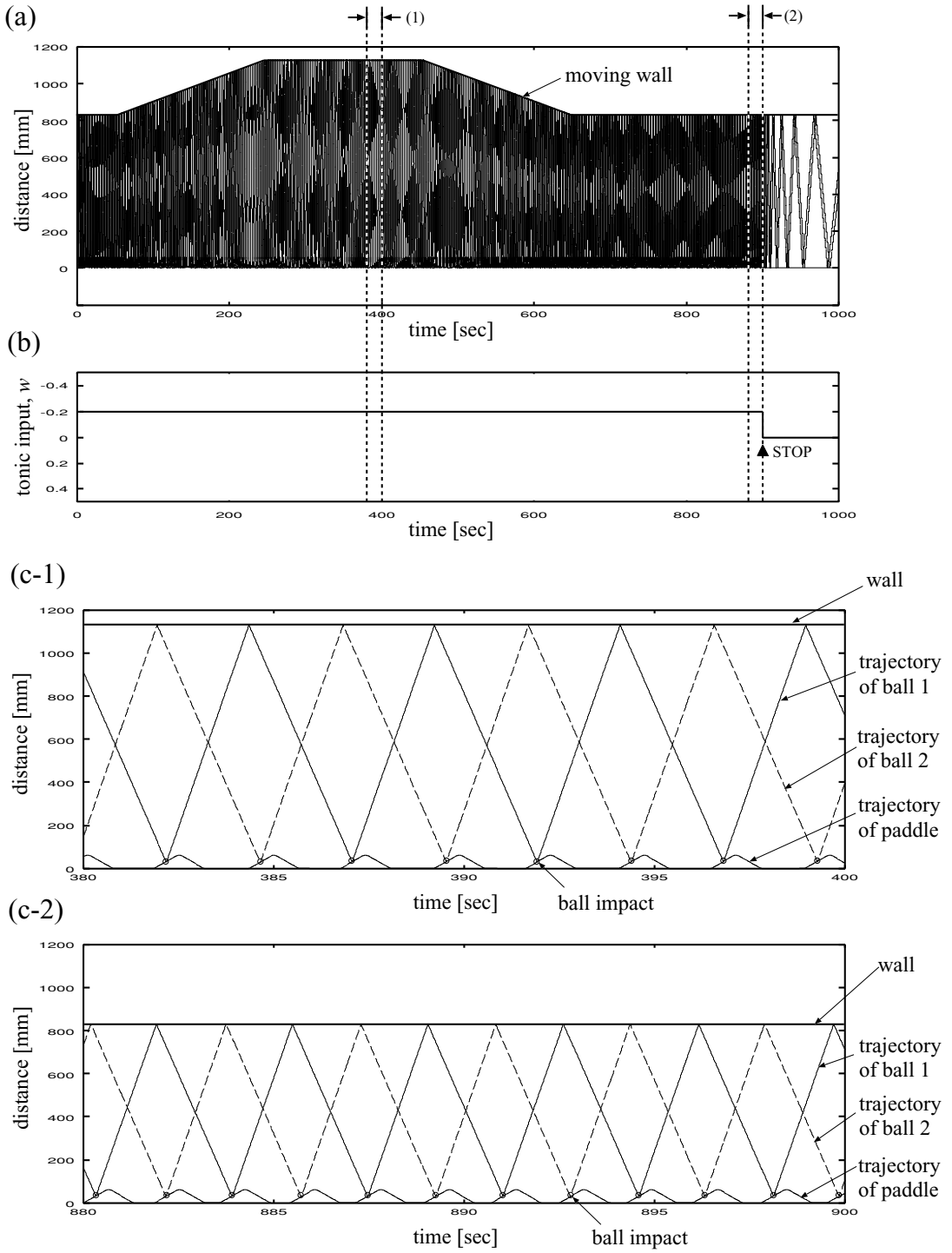

Fig. 11. Effect of three timing-control mechanisms in the moving-wall-bouncing task (ex.3): (a) the whole chart of the trajectories of the paddle and two balls. This graph shows how the wall moves; (b) the change of the tonic input w which is a higher-level command of the Brain System. At 900 seconds, the tonic input is switched from -0.2 to 0.0. $w = 0$ means the higher-level command *stop*; (c-1) the enlargement of the region (1) in (a); and (c-2) the enlargement of the region (2) in (a). (c-1) and (c-2) show the details of the trajectories of the paddle and two balls.

traditional robots, but is able to adapt to the environment by exploiting the above-mentioned mechanisms based on interaction with the environment.

IV. HUMAN PERFORMANCE MEASUREMENT

A subject was instructed to always look at the neighbourhood of the wall and to hit a ball repeatedly against a wall (Fig. 12). The ball rolls or slides on a horizontal guide and rebounds off the wall. The distance between the ball's impact point and the wall is about 215 mm. Three colored markers were attached to the subject's shoulder, elbow and the paddle. These markers were recorded in the sagittal plane with a digital video camera, and the position, velocity and acceleration of each marker were calculated from the recorded data.

https://doi.org/10.1017/S0263574705002110 Published online by Cambridge University Press

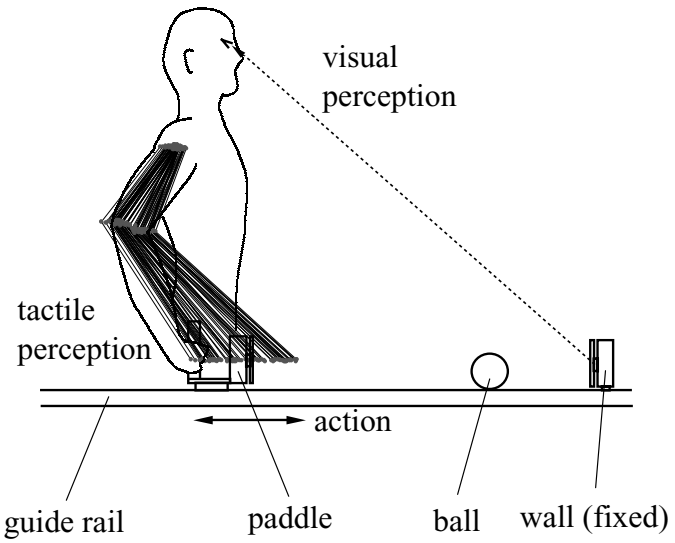

Fig. 12. The experimental setup in the human performance measurement. A subject hits a ball repeatedly against a wall, looking at the neighbourhood of the wall. The ball rolls on a horizontal guide and rebounds off the wall. Three colored markers which are attached to the subject's shoulder, elbow and the paddle are recorded in the sagittal plane with a digital video camera.

Figure 13(a) shows the three dimensional plot of the paddle's movemnet in the phase space whose axes are position, velocity and acceleration, and Figs 13(b)∼(d) show the phase plane plots of the paddle's movement in (b) velocity vs. position, (c) acceleration vs. velocity and (d) acceleration vs. position. The open circles denote the ball's impacts. We can confirm that the trajectory of the paddle settles down to a certain fixed limit cycle and that the ball's impacts gather in a specific region. Figure 14 clarifies the characteristics of this specific region. The right graph (b) in Fig. 14 is the enlargement of the region around the ball's impacts in the left graph (a). The horizontal line is time and the vertical line is the operation parameter $\ddot{x}_p/(\dot{x}_p)^2$, which is closely related to the open-loop stability of the system. Each impact point is arranged on the time 0 as a standard. The motion of the paddle gathers quickly at about 0.05 seconds before the ball's impact. The shaded area is the open-loop stable region given by Equation (12). We substituted the values, $L = 215$ mm and $e_p = e_w = 0.8$, into Equation (12) and obtained the condition for open-loop stability. In this experiment, the range of open-loop stability is $-0.0047 < \ddot{x}_p/(\dot{x}_p)^2 < 0.021$. All impacts exist within this range in which the motion of the ball is stabilized passively. This means that humans may exploit the open-loop stability for stable control of a ball in the wall-bouncing task. This result corresponds to the hypothesis shown by Sternad et al. in the one-handed ball bouncing task.[20] The fact that the ball impacts gather around $\ddot{x}_p/(\dot{x}_p)^2 = 0$ means that the "open-loop stable mechanism" may realize the wall-bouncing task without the environmental parameters.

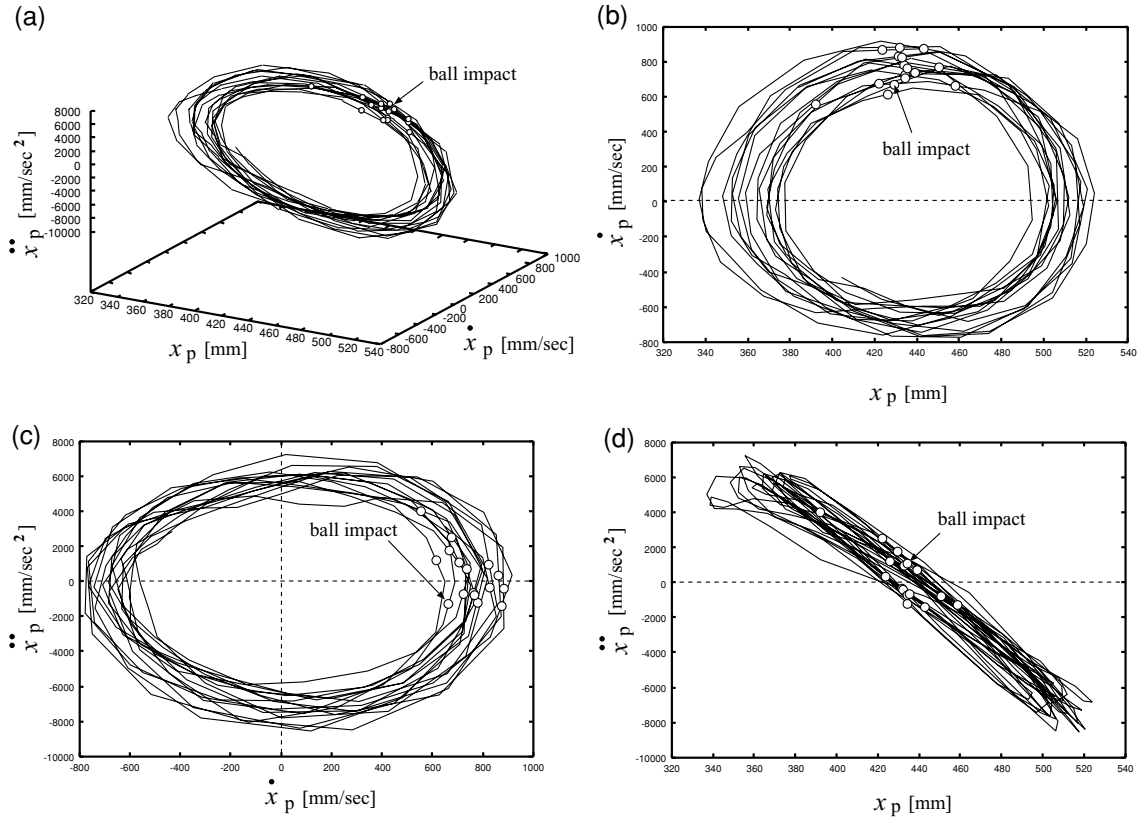

Fig. 13. The paddle's trajectories and ball impacts in the wall-bouncing task (human performance measurement): (a) three dimensional phase-space plot in acceleration vs. velocity vs. position; (b) phase-plane plot in velocity vs. position; (c) phase-plane plot in acceleration vs. velocity; and (d) phase-plane plot in acceleration vs. position.

https://doi.org/10.1017/S0263574705002110 Published online by Cambridge University Press

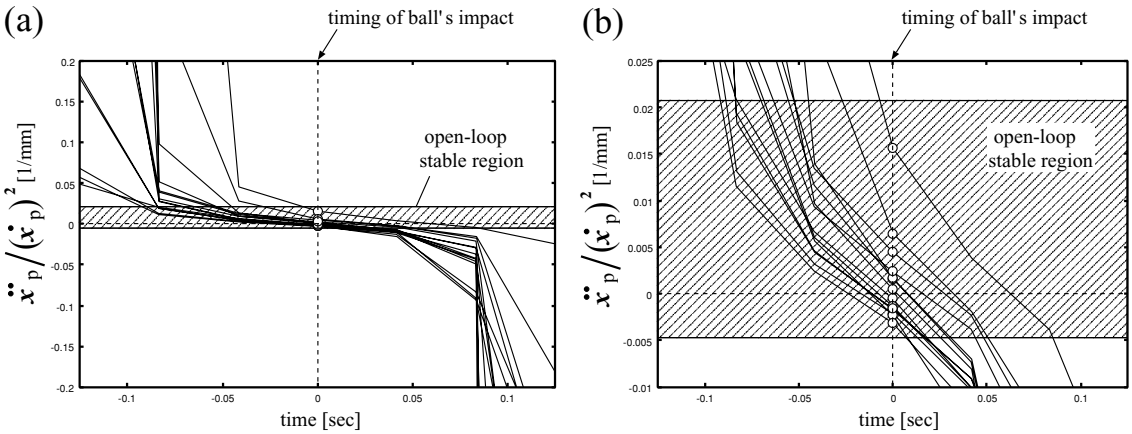

Fig. 14. Ball impacts gathering into the open-loop stable region (human performance measurement): (a) the paddle's trajectories and the ball's impacts; (b) the enlargement of the region around the ball's impacts in (a). The horizontal line is time and the vertical line is the operation parameter $\ddot{x}_p/(\dot{x}_p)^2$. Each impact point is arranged on the time 0 as the standard. The shaded area is the open-loop stable region given by Equation (12). All impact points exist within the range of open-loop stability.

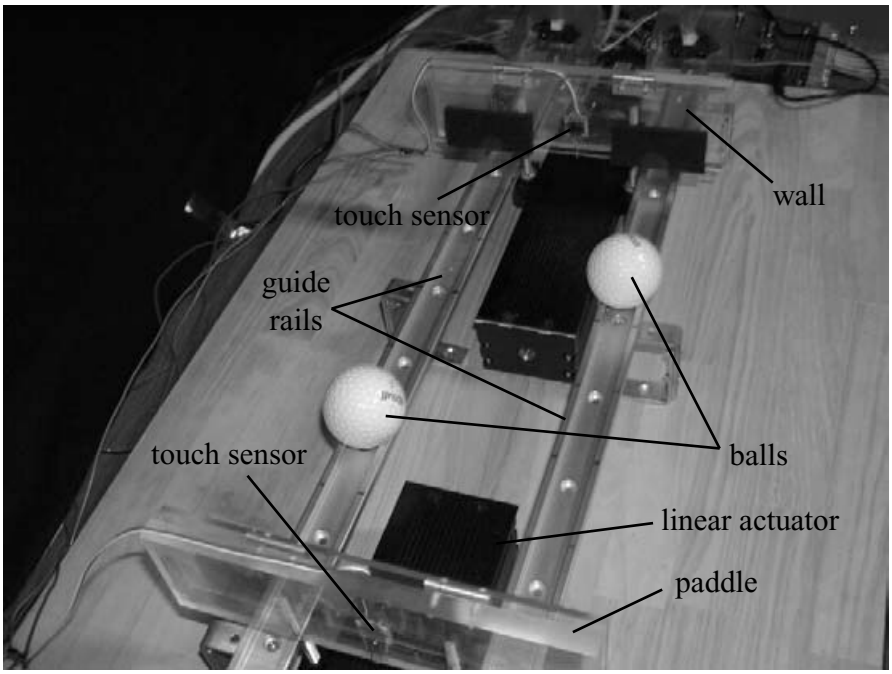

Fig. 15. Wall-bouncing-juggling robot. The linear actuator drives the paddle back and forth and the paddle hits two balls at the appropriate timing. Two balls respectively roll on the two, horizontal and parallel guide rails. The touch sensors are attached to the paddle and the wall, and only the timing of the ball's contact with the paddle and the wall is detectable.

V. ROBOT EXPERIMENT

We made a robot perform the wall-bouncing-juggling task, in which a robot repeats the action of hitting two balls rebounding off the wall (Fig. 15). The linear actuator drives the paddle back and forth and the paddle hits two balls at the appropriate timing. The two horizontal guide rails are arranged in parallel along the single axis in which the paddle can move, and each ball rolls on the separate guide rail. The distance between the robot and the wall is about 250 mm. The touch sensors are attached to the robot's paddle and the wall, and only the timing of the ball's contact with the paddle and the wall is detectable while the robot can not distinguish one ball from the other. As mentioned in Section III.1, the act of hitting a ball with a fixed velocity at a fixed position stabilizes the ball's motion passively. To satisfy the condition for open-loop stability, the robot's paddle is driven with a fixed velocity, $V_p = 300$ mm/sec, at the point of impact. Moreover, we fixed the coupling coefficient parameters of the BFC robotic rhythm oscillator as $\delta_1 = \delta_3 = 0.1$, $\delta_2 = -0.1$. The tonic input parameter w was fixed as $w = -0.05$.

To show the environmental adaptability, we gradually changed the angle of the slope. Figure 16 displays a sequence of the video in this task. Although the change of the slope angle leads to the change of the interval between ball's impacts, the robot can continue to hit two balls keeping the relationship between balls. Figure 17 shows three kinds of data: (1) the membrane potentials of each oscillator

https://doi.org/10.1017/S0263574705002110 Published online by Cambridge University Press

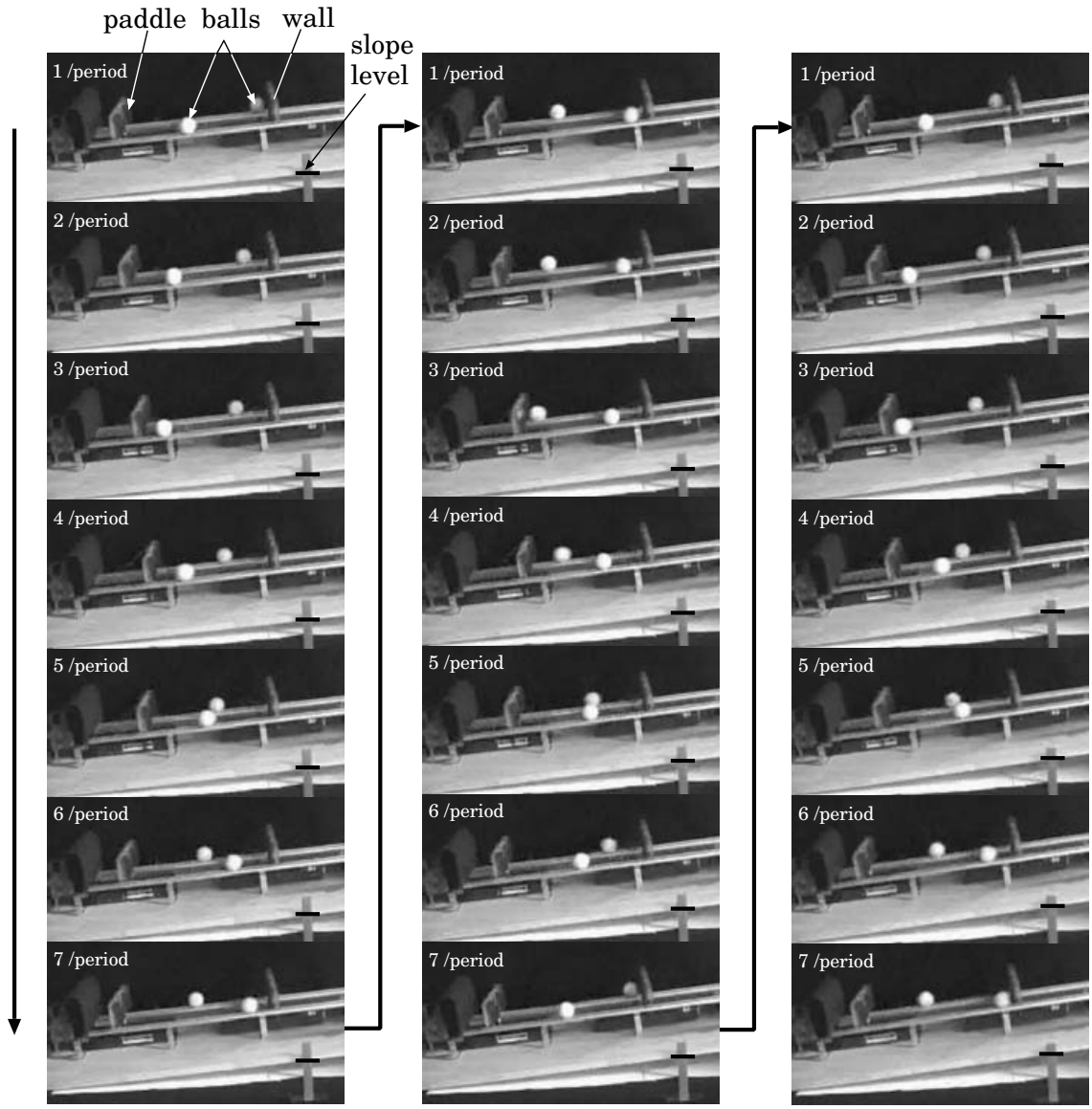

Fig. 16. The sequence of the video in the wall-bouncing-juggling task with a moving slope. (robot experiment): Even if angle of slope change, the robot can continue to hit two balls keeping the relationship between balls.

constituting the BFC robotic rhythm oscillator of the robot, (2) the input signals of touch sensors on the paddle and the wall, and (3) the two balls' trajectories. The rhythm core oscillator (osc0), the sensor ocillator 1 (osc1), and the motor oscillator (osc3) mutually synchronize in phase, while the sensor oscillator 2 (osc2) reciprocally synchronizes the other oscillators out of phase. Two balls' motion also synchronize out of phase. These motions, which are the self-organized temporal pattern of the whole system, emerge from the interaction between the robot and the environment. The important point is replacing the continuous problem to generate the motion for hitting balls with the discrete problem about the timing of the ball impact. The discrete rhythm information of motion is transmitted to the robot itself through the environment (a ball), permitting the robot to self-organize its motion through discrete coupling (weak coupling). As a result, the robot can recover and perform the stable wall-bouncing-juggling task even if the angle of the slope changes.

VI. CONCLUSION

We proposed a hierarchical architecture suited to a juggling-like task involving sensory-motor coordination. Using the proposed BFC robotic rhythm oscillator, we realized a robot which can juggle two balls rebounding off the wall and confirmed that the robot autonomously generates stable rhythmic movement without any global synchronization or control, due to the local interaction of the oscillators and their entrainment properties. The BFC robotic rhythm oscillator can be interpreted as a system inspired by two mechanisms – the reflex generated by perception, and CPGs. We know that the CPG can modify the reflex pattern by using sensor inputs as well as higher-level brain commands.[23,24] The reflex here can be regarded as a solution of inverse kinematics, because the motion pattern is fixed in our system. The BFC robotic rhythm oscillator autonomously acquires this solution due to the oscillator's entrainment property. This paper especially focused on the following features of the proposed architecture for

https://doi.org/10.1017/S0263574705002110 Published online by Cambridge University Press

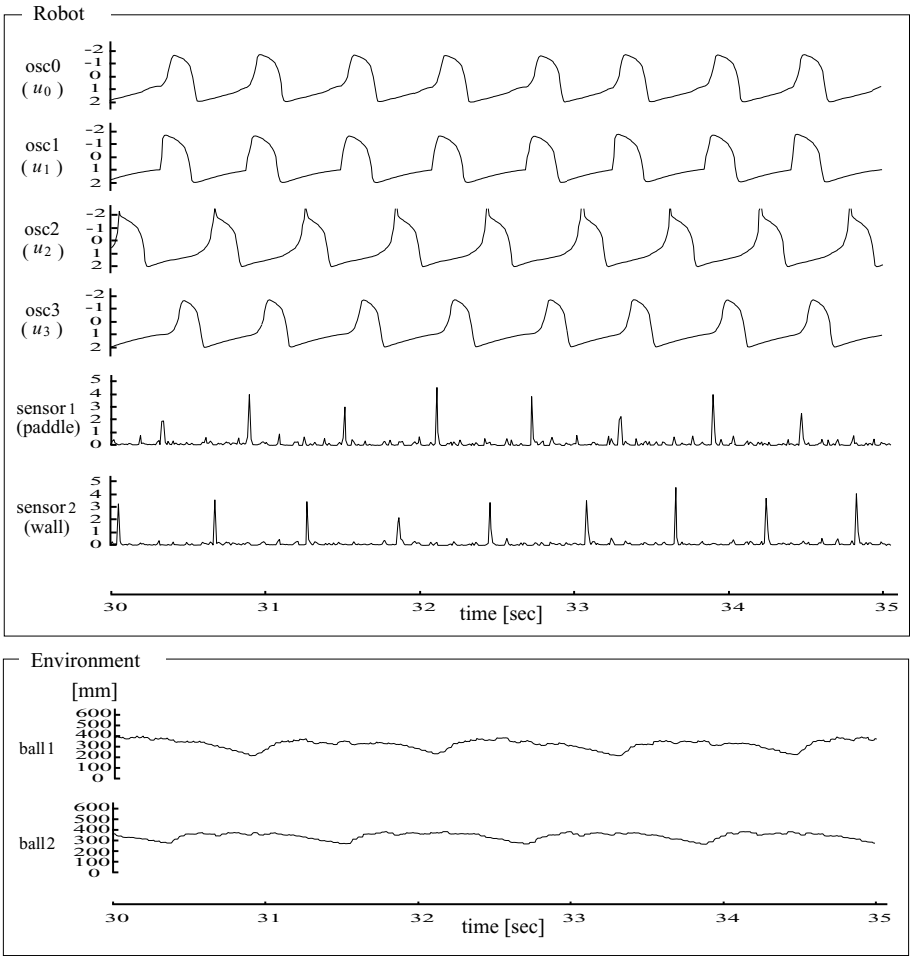

Fig. 17. BFC robotic rhythm oscillator self-organizes through the environment. (robot experiment): The upper graphs show two kinds of data: the membrane potentials of each oscillator constituting the BFC robotic rhythm oscillator; and the input signals of touch sensors on the paddle and the wall. The lower graphs show the two balls' trajectories.

rhythmic movement generation: (1) The motion emerging from the local interaction of the oscillators and entrainment (weak coupling) leads to stable performance of the whole system; and (2) Two passive-control mechanisms, which are the "entrainment mechanism" and the "open-loop stable mechanism," guarantee the dynamic stability of the whole system including the robot and the environment. As a result, the stable rhythmic motion emerges as the dynamic temporal pattern in the whole system. The rhythm of motion between the robot and the environment self-organizes through discrete information about the environment, and the self-organized timing selection leads to the successful task.

Our results also suggest the importance of kinetic information (timing information) about the impact in rhythmic movement. Amazeen et al. studied the timing selection of rhythmic catching in human behavior.[19] They revealed a constant time interval between the zenith of the ball's trajectory and the initiation of the catch from an analysis of the hand's trajectory. They subsequently hypothesized that humans may use time-to-contact information about the ball's zenith to time the catch appropriately. Sternad et al. also studied the one-handed bouncing ball task, in situations which excluded various kinds of perceptual information.[20] They concluded that kinetic information about the impact is more necessary than visual information, although the latter gives information about the continuous kinetic trajectory of the ball. Moreover, it is known that expert jugglers depend more on the sensation achieved by contact between the hand and balls, whereas novice jugglers rely predominantly on their eyes.[25] This shows that tactile information about the ball contact can substitute for visual information. Our results are consistent with this knowledge of human behavior, because only two timings at the moment of the ball's contact with either the paddle or the wall are used as perceptual information. Timing information about the impact provides the most important information needed to achieve dynamic stability.[26–28]

In future work, we will consider the following two themes: At first, we should add a more functional mechanism at higher levels in our Brain System. We demonstrated an example of global order between the robot and the environment. However, a generated temporal pattern is not always a pattern suited to the task. A stable pattern does not necessarily mean that the task is accomplished successfully. In this paper, we noted that our architecture makes the whole system stable if the proposed BFC robotic rhythm oscillator is well-tuned for the task. In general, a robot needs the capability to judge whether it is performing the task successfully or not. A function at higher levels may help to generate an optimal motion pattern which is always able to accomplish the task.

https://doi.org/10.1017/S0263574705002110 Published online by Cambridge University Press

Secondly, we should realize a sequence of motion patterns such as a real juggling trick. We discussed the stability of a single motion pattern. At the next step, we will relate some motion patterns to each other and realize a smooth transition from one behavior attractor to another. It may be useful to exploit a bifurcation of nonlinear system dynamics with a change in a control parameter. We will show that various motion patterns emerge as stable limit cycles generated by the global entrainment between the limbs, the neural system, and the environment. And we will claim that the "bidirectional weak coupling" approach is useful for the timing selection essential to dynamic dexterity.

References

1. J. Ayers, J. L. Davis and A. Rudolph, *Neurotechnology for Biomimetic Robots* (MIT Press, 2002).
2. J. B. Buck and E. Buck, "Biology of Synchronous Flashing of Fireflies," *Nature* **211**, 526–564 (1966).
3. G. Schöner and J. A. S. Kelso, "Dynamics Pattern Generation in Behavioral and Neural Systems," *Science* **239**, 1513–1520 (1988).
4. J. A. S. Kelso, *Dynamic Pattern: The Self-Organization of Brain and Behaviour* (MIT Press 1995).
5. S. H. Strogatz and I. Stewart, "Coupled Oscillators and Biological Shynchronization," *Scientific American*, 68–75 (Dec., 1993).
6. E. Thelen and L. B. Smith, *A Dynamic Systems Approach to the Development of Cognition and Action* (MIT Press, 1994).
7. R. FitzHugh, "Impulses and Physiological States in Theoretical Models of Nerve Membrane," *Biophysical Journal* **1**, 445–466 (1961).
8. K. Yoshino, T. Nomura, K. Pakdaman and S. Sato, "Synthetic analysis of periodically stimulated excitable and oscillatory membrane models," *Physical Review E* **59**(1), 956–969 (1999).
9. S. Miyakoshi, M. Yamakita and K. Furuta, "Juggling Control Using Neural Oscillator," *Proc. IEEE International Conference on Intelligent Robots and Systems* **2**, 1186–1193 (1994).
10. Matthew M. Williamson, "Neural Control of Rhythmic Arm Movements," *Neural Networks Special Issue on Neural Control of Movement* **11**, 1379–1394 (1998).
11. S. Schaal and D. Sternad, "Programmable Pattern Generators," *Proc. International Conference on Computational Intelligence in Neuroscience* (1998) pp. 48–51.
12. S. Schaal, S. Kotosaka and D. Sternad, "Nonlinear Dynamical Systems as Movement Primitives," *Proc. IEEE International Conference on Humanoid Robotics* (2000) CD.
13. G. Taga, "A model of the neuro-musculo-skeletal system for human locomotion: I. Emergence of basic gait," *Biological Cybernetics* **73**, 97–111 (1995).
14. G. Taga, "A model of the neuro-musculo-skeletal system for human locomotion: II. Real-time adaptability under various constraints," *Biological Cybernetics* **73**, 113–121 (1995).
15. S. Schaal, C. G. Atkson and D. Sternad, "One-Handed Juggling: A Dynamical Approach to a Rhythmic Movement Task," *Journal of Motor Behavior* **28**(2), 165–183 (1996).
16. H. Hirai and F. Miyazaki, "A Bidirectional Weak Coupling Approach To Rhythmic Movement," *International Symposium on Adaptive Motion of Animals and Machines* (2003) CD. WeP 11–3.
17. H. Hirai and F. Miyazaki, "Rhythmic Movement by Neural Oscillator with Periodic Stimulus," *Proc. IEEE International Conference on Robotics and Automation* (2003) **Vol. 1**, pp. 226–231.
18. H. Hirai and F. Miyazaki, "What Are Key Mechanisms for Adaptive Wall-Bouncing Control?", *Proc. IEEE International Conference on Robotics and Biomimetics* (2004) CD. No. 318.
19. E. L. Amazeen, P. G. Amazeen, A. A. Post and P. J. Beek, "Timing the Selection of Information During Rhythmic Catching," *Journal of Motor Behavior* **31**(3), 279–289 (1999).
20. D. Sternad, M. Duarte, H. Katsumura and S. Schaal, "Dynamics of a Bouncing Ball in Human Performance," *Physical Review E* **63**, 011902-1–011902-8 (2000).
21. R. A. Schmidt, T. D. Lee, *Motor Control and Learning: A Behavioural Emphasis* (Human Kinetics, 1998).
22. M. Buehler, D. E. Koditschek and P. J. Kindlmann, "Planning and Control of Robotic Juggling and Catching Tasks," *Int. J. of Robotic Research* **13**(9), 101–118 (1994).
23. M. L. Shik, F. V. Severin and G. N. Orlovskii, "Control of walking and running by means of electrical stimulation of mid-brain," *Biophysics* **11**(4), 659–666 (1966).
24. S. Grillner and P. Wallen, "On peripheral control mechanisms acting on the central pattern generators for swimming in the dogfish," *Journal of Experimental Biology* **98**, 1–22 (1982).
25. P. J. Beek and A. Lewbel , "The Science of Juggling," *Scientific American* **273**(5), 92–97 (1995).
26. S. Schaal and C. G. Atkson, "Open Loop Stable Control Strategies for Robot Juggling," *Proc. IEEE International Conference on Robotics and Automation* (1993) **Vol. 3**, pp. 913–918.
27. H. Cruse, "What mechanisms coordinate leg movement in walking arthropods?", *Trends in Neuro-science* **13**(1), 15–21 (1990).
28. M. Takeuchi, M. Matsushima, M. Kawatani, T. Hashimoto and F. Miyazaki, "Dynamic Dexterity for the Performance of Wall-Bouncing Tasks," *Proc. IEEE International Conference on Robotics and Automation* (2002) **Vol. 5**, pp. 1559–1564.

APPENDIX

A. Ball's motion under gravity and friction

We explain the wall-bouncing task with a slope angle of α. A ball rolls along a slope and rebounds off a wall. In this section, we consider the effects of gravity, friction and ball rotation. Below, we divide the ball's cyclic motion into four phases and explain its motion in each phase (Fig. 18).

1) *The motion of a ball at the point of contact with the paddle:* Let the variables $\dot{x}^n_{b1,p}$ and $\dot{x}^n_{b2,p}$ be the velocities of a ball immediately before and after the nth ball's contact with the paddle, the variable V_p be the constant velocity of the paddle at the point of the ball's contact, and e_p be the coefficient of restitution of the paddle. Then, using the restitution equation, the ball's velocity immediately after the nth impact is described by

$$\begin{aligned}\dot{x}^n_{b2,p} &= -e_p\dot{x}^n_{b1,p} + (1+e_p)V_p \\ &= s_1\left(\dot{x}^n_{b1,p}\right)\end{aligned} \tag{20}$$

where s_1 denotes a function of $\dot{x}^n_{b1,p}$.

2) *The motion of a ball rolling up along a slope:* After the nth ball's contact with the paddle, a ball rolls up along a slope with the following initial state:

$$x_{bu}(0) = 0 \tag{21}$$

$$\dot{x}_{bu}(0) = \dot{x}^n_{b2,p} \tag{22}$$

where $x_{bu}(0)$ and $\dot{x}_{bu}(0)$ denote the initial position and velocity of the ball. Let the variables t, g, μ', α and L be time, the acceleration of gravity, the coefficient of kinetic friction, the angle of a slope and the distance between the

https://doi.org/10.1017/S0263574705002110 Published online by Cambridge University Press

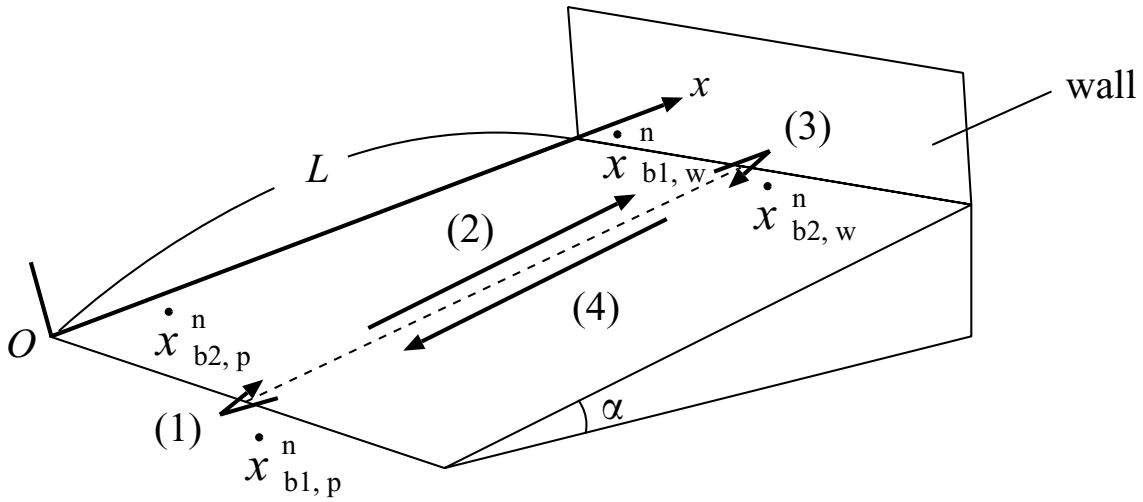

Fig. 18. Four phases of ball's cyclic motion in the wall-bouncing task with a slope: (1) the motion of a ball at the point of contact with the paddle; (2) the motion of a ball rolling up along a slope; (3) the motion of a ball at the point of contact with the wall; and (4) the motion of a ball rolling down along a slope.

wall and the paddle's ideal impact point, m and r be the mass and radius of the ball, and $\ddot{x}_{bu}(t)$ and $\ddot{\theta}_{bu}(t)$ be the acceleration and angular acceleration of the ball at the time t respectively. The ball's moment of inertia, I, is given by $I = \frac{2}{5}mr^2$. Then, the motion of the ball is expressed as the following equations:

$$m\ddot{x}_{bu}(t) = -mg\sin\alpha - \mu' mg\cos\alpha \tag{23}$$

$$I\ddot{\theta}_{bu}(t) = -r\mu' mg\cos\alpha \tag{24}$$

From Equations (21), (22), (23) and (24), we can obtain the velocity of a ball immediately before the nth ball's contact with the wall, $\dot{x}^n_{b1,w}$ as below:

$$\dot{x}^n_{b1,w} = \dot{x}_{bu}(t)|_{x_{bu}(t)=L} = s_2\left(\dot{x}^n_{b2,p}\right) \tag{25}$$

where $\dot{x}_{bu}(t)|_{x_{bu}(t)=L}$ is the ball's velocity at the moment of the ball's position $x_{bu}(t) = L$, and s_2 is a nonlinear function of $\dot{x}^n_{b2,p}$.

3) *The motion of a ball at the point of contact with the wall:* Let the variable $\dot{x}^n_{b2,w}$ be the velocities of the ball immediately after the nth ball's contact with the wall. Then, using the restitution equation, $\dot{x}^n_{b2,w}$ is described as the following equation:

$$\begin{aligned}\dot{x}^n_{b2,w} &= -e_w\dot{x}^n_{b1,w} \\ &= s_3\left(\dot{x}^n_{b1,w}\right)\end{aligned} \tag{26}$$

where s_3 is a function of $\dot{x}^n_{b1,w}$.

4) *The motion of a ball rolling down along a slope:* After the nth ball's contact with the wall, it rolls down along a slope with the following initial state:

$$x_{bd}(0) = L \tag{27}$$

$$\dot{x}_{bd}(0) = \dot{x}^n_{b2,w} \tag{28}$$

where $x_{bd}(0)$ and $\dot{x}_{bd}(0)$ are the initial position and velocity of the ball. Let the variables $\ddot{x}_{bd}(t)$ and $\ddot{\theta}_{bd}(t)$ be the acceleration and angular acceleration of the ball at the time of t. Then, its motion is expressed in the following equations:

$$m\ddot{x}_{bd}(t) = -mg\sin\alpha + \mu' mg\cos\alpha \tag{29}$$

$$I\ddot{\theta}_{bd}(t) = r\mu' mg\cos\alpha \tag{30}$$

From Equations (27), (28), (29) and (30), we can obtain the ball's velocity immediately before the $n+1$th ball's contact with the paddle, $x^{n+1}_{b1,p}$.

$$\dot{x}^{n+1}_{b1,p} = \dot{x}_{bd}(t)|_{x_{bd}(t)=0} = s_4\left(\dot{x}^n_{b2,w}\right) \tag{31}$$

where $\dot{x}_{bd}(t)|_{x_{bd}(t)=0}$ is the ball's velocity at the moment of the ball's position $x_{bd}(t) = 0$, and s_4 is a nonlinear function of $\dot{x}^n_{b2,w}$.

From the above-mentioned ball's motion in each phase, the ball's whole motion in a cycle is given below:

$$\dot{x}^{n+1}_{b1,p} = s_4 \circ s_3 \circ s_2 \circ s_1\left(\dot{x}^n_{b1,p}\right) \tag{32}$$

where $s_4 \circ s_3 \circ s_2 \circ s_1$ denotes the composition function $s_4(s_3(s_2(s_1(\cdot))))$.

Let us replace $\dot{x}^n_{b1,p}$ with $\dot{x}^n_b$. Then, the subsequent sequence $\{\dot{x}^n_b\}$ is rewritten as the following equations:

$$\dot{x}^1_b \leq 0 \tag{33}$$

$$\begin{aligned}\dot{x}^{n+1}_b &= -\sqrt{\left(a\dot{x}^n_b + b\right)^2 + c} \\ &(-1 < a < 0, b > 0, c > 0)\end{aligned} \tag{34}$$

where a, b, c are nonlinear functions of e_w, e_p, V_p, α and so on. These parameters of Equation (34) are separated into the following three cases according to the coefficient of static friction μ, the coefficient of kinetic friction μ' and a slope angle α.

https://doi.org/10.1017/S0263574705002110 Published online by Cambridge University Press

$0 \le \tan\alpha < \frac{7}{2}\mu'$:

$$a = -\sqrt{k_1 k_2}\, e_w e_p \tag{35}$$

$$b = \sqrt{k_1 k_2}\, e_w (1 + e_p) V_p \tag{36}$$

$$c = \frac{10}{7} g L \sin\alpha \{1 - (\sqrt{k_1 k_2}\, e_w)^2\} \tag{37}$$

$$k_1 = \frac{5}{7} - \frac{10}{7} \frac{2g\sin\alpha + 12\mu' g\cos\alpha}{(2g\sin\alpha + 7\mu' g\cos\alpha)^2} \mu' g \cos\alpha \tag{38}$$

$$(0 < k_1 < 1)$$

$$k_2 = \frac{5}{7} - \frac{10}{7} \frac{-2g\sin\alpha + 12\mu' g\cos\alpha}{(2g\sin\alpha - 7\mu' g\cos\alpha)^2} \mu' g \cos\alpha \tag{39}$$

$$(0 < k_2 < 1)$$

$\frac{7}{2}\mu' \le \tan\alpha < \frac{7}{2}\mu$:

$$a = -\sqrt{k_1 k_2}\, e_w e_p \tag{40}$$

$$b = \sqrt{k_1 k_2}\, e_w (1 + e_p) V_p \tag{41}$$

$$c = \frac{10}{7} g L \sin\alpha \{1 - (\sqrt{k_1 k_2}\, e_w)^2\} \tag{42}$$

$$k_1 = \frac{5}{7} - \frac{10}{7} \frac{2g\sin\alpha + 12\mu' g\cos\alpha}{(2g\sin\alpha + 7\mu' g\cos\alpha)^2} \mu' g \cos\alpha \tag{43}$$

$$(0 < k_1 < 1)$$

$$k_2 = \frac{5}{7} \quad (0 < k_2 < 1) \tag{44}$$

$\frac{7}{2}\mu \le \tan\alpha \le 1$:

$$a = -e_w e_p \tag{45}$$

$$b = e_w (1 + e_p) V_p \tag{46}$$

$$c = 2gL\sin\alpha \left\{ \left(1 - e_w^2\right) - \frac{\mu'}{\tan\alpha}\left(1 + e_w^2\right) \right\} \tag{47}$$

B. Global stability of equations (18) and (19)

We can prove the global stability of the system under conditions considering the effects of gravity, friction and ball rotation. It is only necessary to prove the following proposition:

Proposition. *Let the variables* $\boldsymbol{N}$ *and* $\boldsymbol{R}$ *be the sets of natural numbers and real numbers, the subsequent sequence* $\{\dot{x}_b^n \mid n \in \boldsymbol{N},\ \dot{x}_b^n \in \boldsymbol{R}\}$ *be defined as follows:*

$$\dot{x}_b^1 \le 0 \tag{48}$$

$$\dot{x}_b^{n+1} = -\sqrt{\left(a\dot{x}_b^n + b\right)^2 + c} \tag{49}$$

$$(-1 < a < 0, b > 0, c > 0)$$

Then, $\{\dot{x}_b^n\}$ *always converges at a certain value.*

Proof. Since $\dot{x}_b^n = \{\dot{x}_b^n \mid n \in \boldsymbol{N}, \dot{x}_b^n \in \boldsymbol{R}\}$, we can obtain the following inequality from Equation (49).

$$\dot{x}_b^n < 0 \quad \text{for } \forall n \in \boldsymbol{N} \tag{50}$$

On the other hand, the difference between $(\dot{x}_b^{n+1})^2$ and $(\dot{x}_b^n)^2$ can be expressed as

$$\left(\dot{x}_b^{n+1}\right)^2 - \left(\dot{x}_b^n\right)^2 = -(1 - a^2)\left(\dot{x}_b^n - \frac{ab}{1 - a^2}\right)^2 + \frac{b^2 + c - a^2 c}{1 - a^2} \tag{51}$$

Let us define the variable M as $M = \frac{ab - \sqrt{b^2 + c - a^2 c}}{1 - a^2}$, which is a solution of the equation $(\dot{x}_b^{n+1})^2 - (\dot{x}_b^n)^2 = 0$, and divide the domain $(-\infty, 0)$ into two subsets, I_1 and I_2, by the variable M.

$$I_1 = (-\infty, M] \tag{52}$$

$$I_2 = [M, 0) \tag{53}$$

Then,

$$\{\dot{x}_b^n\}_{n \in \boldsymbol{N}} \subset I_1 \Rightarrow \dot{x}_b^n \le \dot{x}_b^{n+1} \tag{54}$$

$$\{\dot{x}_b^n\}_{n \in \boldsymbol{N}} \subset I_2 \Rightarrow \dot{x}_n \ge \dot{x}_b^{n+1} \tag{55}$$

where, note $\{\dot{x}_b^n\}_{n \in N} < 0$. Since $\dot{x}_b^n \le M (< 0)$ is always satisfied for $\forall \dot{x}_b^n \in I_1$, the following condition is obtained:

$$\begin{aligned} \dot{x}_b^{n+1} &= -\sqrt{\left(a\dot{x}_b^n + b\right)^2 + c} \\ &\le -\sqrt{(aM + b)^2 + c} = M (\in I_1) \end{aligned} \tag{56}$$

Similarly, since $M \le \dot{x}_b^n (< 0)$ is satisfied for $\forall \dot{x}_b^n \in I_2$, the following condition is given:

$$\begin{aligned} \dot{x}_b^{n+1} &= -\sqrt{\left(a\dot{x}_b^n + b\right)^2 + c} \\ &\ge -\sqrt{\left(aM + b\right)^2 + c} = M (\in I_2) \end{aligned} \tag{57}$$

Equation (54) means that the subsequent sequence $\{\dot{x}_b^n \mid \forall \dot{x}_b^n \in I_1\}$ is a monotonically increasing sequence and Equation (56) means this sequence is bounded from above. Applying the following Lemma 1:

Lemma 1. *Let the variable* $\{X_n\}_{n \in \boldsymbol{N}}$ *be a real number sequence. If the subsequent sequence* $\{X_n\}_{n \in \boldsymbol{N}}$ *is bounded from above by a certain real number U and is a monotonically increasing sequence,* $\{X_n\}_{n \in \boldsymbol{N}}$ *converges at its supremum:*

$$X_k \le X_{k+1} \le U \Rightarrow \lim_{n \to \infty} X_n = \sup\{X_n \mid n \in \boldsymbol{N}\} \quad \text{for } \{X_n\}_{n \in \boldsymbol{N}} \in \boldsymbol{R},\ \forall k \in \boldsymbol{N},\ \exists U \in \boldsymbol{R} \tag{58}$$

where $\sup\{\cdot\}$ *denotes the supremum of a set* $\{\cdot\}$,
we can obtain

$$\lim_{n \to \infty} \left\{\dot{x}_b^n \middle|\ n \in \boldsymbol{N}\right\} = M\left(= \sup\left\{\dot{x}_b^n \middle|\ n \in \boldsymbol{N}\right\}\right) \quad \text{for } \left\{\dot{x}_b^n\right\} \subset I_1 \tag{59}$$

https://doi.org/10.1017/S0263574705002110 Published online by Cambridge University Press

Similarly, Equation (55) shows that the subsequent sequence $\{\dot{x}_b^n |\ \forall \dot{x}_b^n \in I_2\}$ is a monotonically decreasing sequence and Equation (57) means this sequence is bounded from below. Applying the following Lemma 2:

Lemma 2. *Let the variable* $\{X_n\}_{n\in \boldsymbol{N}}$ *be a real number sequence. If the subsequent sequence* $\{X_n\}_{n\in \boldsymbol{N}}$ *is bounded from below by a certain real number* L *and is a monotonically decreasing sequence,* $\{X_n\}_{n\in \boldsymbol{N}}$ *converges at its infimum:*

$$X_k \geq X_{k+1} \geq L \Rightarrow \lim_{n\to\infty} X_n = \inf\{X_n |\ n \in \boldsymbol{N}\}$$
$$\textit{for } \{X_n\}_{n\in \boldsymbol{N}} \in \boldsymbol{R},\ \forall k \in \boldsymbol{N},\ \exists L \in \boldsymbol{R} \quad (60)$$

where $\inf\{\cdot\}$ *denotes the infimum of a set* $\{\cdot\}$,

we can obtain

$$\lim_{n\to\infty} \left\{\dot{x}_b^n \middle|\ n \in \boldsymbol{N}\right\} = M \left(= \inf\left\{\dot{x}_b^n \middle|\ n \in \boldsymbol{N}\right\}\right) \ \textit{for } \left\{\dot{x}_b^n\right\} \subset I_2 \quad (61)$$

Then, let us define I as

$$I = \bigcup_{n=1,2} I_n = (-\infty, 0) \quad (62)$$

Thus, Equations (59), (61) yield the following equation:

$$\lim_{n\to\infty} \left\{\dot{x}_b^n \middle|\ n \in \boldsymbol{N}\right\} = M \quad \textit{for } \left\{\dot{x}_b^n\right\} \subset I \quad (63)$$

Therefore, the subsequent sequence $\{\dot{x}_b^n\}$ converges at $M = \frac{ab - \sqrt{b^2 + c - a^2 c}}{1 - a^2}$. Q.E.D.

https://doi.org/10.1017/S0263574705002110 Published online by Cambridge University Press